

Joint IRS Location and Size Optimization in Multi-IRS Aided Two-Way Full-Duplex Communication Systems

Christos N. Efrem and Ioannis Krikidis

Abstract—Intelligent reflecting surfaces (IRSs) have emerged as a promising wireless technology for the dynamic configuration and control of electromagnetic waves, thus creating a smart (programmable) radio environment. In this context, we study a multi-IRS assisted two-way communication system consisting of two users that employ full-duplex (FD) technology. More specifically, we deal with the joint IRS location and size (i.e., the number of reflecting elements) optimization in order to minimize an upper bound of system outage probability under various constraints, namely, minimum and maximum number of reflecting elements per IRS, maximum number of installed IRSs, maximum total number of reflecting elements (implicit bound on the signaling overhead) as well as maximum total IRS installation cost. First, the problem is formulated as a discrete optimization problem and, then, a theoretical proof of its NP-hardness is given. Moreover, we provide a lower bound on the optimum value by solving a linear-programming relaxation (LPR) problem. Subsequently, we design two polynomial-time algorithms, a deterministic greedy algorithm and a randomized approximation algorithm, based on the LPR solution. The former is a heuristic method that always computes a feasible solution for which (a posteriori) performance guarantee can be provided. The latter achieves an approximate solution, using randomized rounding, with provable (a priori) probabilistic guarantees on the performance. Furthermore, extensive numerical simulations demonstrate the superiority of the proposed algorithms compared to the baseline schemes. Finally, useful conclusions regarding the comparison between FD and conventional half-duplex (HD) systems are also drawn.

Index Terms—Intelligent reflecting surface, IRS deployment, full-duplex communication, discrete optimization, NP-hardness, linear-programming relaxation, randomized rounding, approximation algorithm.

I. INTRODUCTION

Intelligent reflecting surface (IRS), also known as reconfigurable intelligent surface, has been considered as one of the most effective techniques to cope with the signal blockage in communication networks operating in millimeter-wave (mmWave) frequency bands. IRS is a planar surface which is installed on the walls or ceilings of buildings so as to create virtual line-of-sight (LoS) links between the transmitters and receivers, thus overcoming the physical obstacles between them. In particular, IRS consists of (mostly) passive reflecting elements that can independently induce a controllable phase shift on the incident electromagnetic wave [2]–[4].

This work was co-funded by the European Regional Development Fund and the Republic of Cyprus through the Research and Innovation Foundation, under the projects INFRASTRUCTURES/1216/0017 (IRIDA) and EXCELLENCE/0918/0377 (PRIME). Part of this work will be presented at the IEEE International Conference on Communications (ICC), 2022 [1].

The authors are with the Department of Electrical and Computer Engineering, University of Cyprus, 1678 Nicosia, Cyprus.

Moreover, IRSs are not expected to perform any sophisticated signal processing operations that require radio-frequency (RF) chains, but only the necessary amplitude attenuation and phase rotation of signals via low-power electronic circuits. In other words, high-cost active components (e.g., power amplifiers) are not required, thus leading to low energy consumption and implementation cost. For this reason, IRSs are usually referred to as “nearly-passive” devices. In addition, they have much lower implementation cost than conventional technologies of active transceivers, such as amplify-and-forward, decode-and-forward relays and multiple-input-multiple-output systems [5], [6].

On the other hand, full-duplex (FD) wireless technology has the potential to double the spectral efficiency, compared to its half-duplex (HD) counterpart, by allowing simultaneous transmission and reception within the same frequency band. This can be achieved at the expense of higher implementation complexity due to the required loop-interference cancellation techniques [7]–[9]. Recently, there is a growing interest of the research community in combining IRSs with FD systems in order to exploit their benefits and advantages [10]–[16].

A. Related Work

To begin with, [17] presents an aerial-IRS (AIRS) system architecture in order to enhance the system performance, compared to the conventional terrestrial IRS, by exploiting the high altitude of AIRS. In particular, the authors study the joint optimization of the transmit beamforming of the ground source-node as well as the placement and passive beamforming of the AIRS. In addition, the single-IRS deployment problem (inside a 3-dimensional box), where an access point communicates with multiple users via the IRS, has been investigated in [18]. Specifically, the weighted sum rate maximization problem has been formulated for three multiple access schemes: non-orthogonal multiple access (NOMA), frequency division multiple access (FDMA), and time division multiple access (TDMA). In order to deal with these problems, the authors have used several methods, namely, monotonic optimization, semidefinite relaxation, alternating optimization and successive convex approximation.

Furthermore, the problem of joint IRS deployment, phase-shift design as well as power allocation for maximizing the energy efficiency of a NOMA network has been recently formulated and solved using machine learning methods [19]. As concerns the coverage of an IRS-assisted network with one base station and one user equipment, [20] has examined the IRS placement problem to maximize the cell coverage by optimizing the IRS orientation and horizontal distance

from the base station. Also, the optimal number of reflecting elements for an IRS, assisting the communication between a transmitter and a receiver, has been proposed in [21]. Particularly, the system rate, energy efficiency, and their tradeoff are maximized by taking into consideration the signaling overhead required for the channel estimation and IRS phase-shift configuration.

Moreover, the (single) FD relay location and power optimization problem in a point-to-point (P2P) communication system has already been addressed in [22]–[24]. Finally, [25]–[28] have developed efficient optimization algorithms for the deployment of ground stations in RF and optical satellite networks with site diversity.

B. Main Contributions

In the majority of existing works, the IRS positions are assumed to be known *in advance*. However, IRS locations have a great impact on the overall system performance. As a result, their optimization is extremely important and deserves its own study. In this paper, we design efficient (polynomial-time) algorithms to jointly optimize the location and size (i.e., the number of reflecting elements) of multiple distributed IRSs in a two-way FD communication network. Specifically, the major contributions of this work are the following:

- Extension of the IRS system model introduced in [11] to multi-IRS systems, including not only small-scale fading but also large-scale path loss. In this way, we exploit the *geometric characteristics* (i.e., the distances between users and IRSs) of the wireless network. Specifically, the deployment of multiple IRSs has two attractive features: i) *small-scale diversity* between the reflecting elements of the same IRS, and ii) *large-scale diversity* between the reflecting elements of distinct IRSs.
- Recent works dealing with the IRS deployment often assume a *continuous (bounded/unbounded) area for installing an IRS* (see, for example, [18] and [20]). Unlike previous research, in this article we consider a *predetermined and finite set of available IRS locations*, thus taking into account physical constraints for the IRS positions. This is of great practical interest, since IRSs are usually installed on the facades, walls or ceilings of existing buildings. Nevertheless, if we are interested in installing IRSs within a bounded continuous area, then this region can be divided into a sufficiently large finite number of distinct points (this method is known as discretization). Therefore, the proposed methodology is still applicable.
- Mathematical formulation of a discrete optimization problem in order to minimize an upper bound of system outage probability, which is subject to several constraints: minimum and maximum number of reflecting elements for each IRS, maximum number of installed IRSs, maximum total number of reflecting elements and maximum total IRS installation cost. In addition, a theoretical proof of its computational complexity (*NP-hardness*) is given.
- Furthermore, we construct a *linear-programming relaxation (LPR)* so as to lower bound the optimum value. Then, we develop two polynomial-time algorithms,

namely, a *deterministic greedy algorithm* and a *randomized approximation algorithm*, whose key ingredient is the LPR solution. The first is a heuristic method which always finds a feasible solution to the problem, while the second achieves an approximate solution via randomized rounding. For the randomized algorithm, we also provide *probabilistic performance guarantees* using concentration inequalities (in particular, Hoeffding’s bound).

- Finally, numerical results show the superiority of the proposed algorithms compared to the benchmarks, while *useful comparisons between FD and HD schemes* are provided as well.

C. Outline and Notation

The remainder of this paper is organized as follows. Section II describes the system model, while Section III formulates the optimization problem and studies its computational complexity. Afterwards, Section IV develops and analyzes the proposed optimization algorithms. In addition, numerical results are provided in Section V. Finally, useful conclusions are given in Section VI, while Appendices A and B contain the proofs of some theorems.

Mathematical notation: Italic letters denote (real/complex) scalars, boldface letters represent vectors and matrices, while calligraphic letters stand for sets and events. $|z|$ denotes the absolute value (or magnitude) of a complex number z and $j = \sqrt{-1}$ is the imaginary unit. In addition, $|\mathcal{A}|$ and \mathcal{B}^c represent the cardinality of a set \mathcal{A} and the complement of an event \mathcal{B} , respectively. The Cartesian product of the sets $\{\mathcal{A}_n\}_{n \in \mathcal{N}} = \{\mathcal{A}_1, \dots, \mathcal{A}_N\}$ is denoted by $\times_{n \in \mathcal{N}} \mathcal{A}_n = \mathcal{A}_1 \times \dots \times \mathcal{A}_N$. Moreover, $\mathbf{0}_N$ is the N -dimensional zero vector and $[\cdot]^\top$ stands for the matrix transpose. The symbols \triangleq and \sim mean “equal by definition” and “distributed as”, respectively. Also, $\log(\cdot)$ represents the natural logarithm (i.e., with base e) and $\binom{n}{m} = \frac{n!}{m!(n-m)!}$ is the binomial coefficient. $\Theta(\cdot)$, $O(\cdot)$, $\Omega(\cdot)$ and $o(\cdot)$ are respectively the big-theta, big-oh, big-omega and little-oh asymptotic notation. Furthermore, the floor and ceiling functions are denoted by $\lfloor \cdot \rfloor$ and $\lceil \cdot \rceil$, respectively. For every $x \geq 0$, $\text{frac}(x) = x - \lfloor x \rfloor$ is the fractional part of x , with $\text{frac}(x) \in [0, 1)$, and $\text{round}(x) = \lfloor x + 0.5 \rfloor$. In addition, $\Pr(\cdot)$ and $\mathbb{E}(\cdot)$ denote probability and expectation (or expected value), respectively. Finally, $\text{Uniform}(\mathcal{D})$ stands for the continuous/discrete uniform distribution on the set \mathcal{D} .

II. SYSTEM MODEL

In this paper, we deal with a multi-IRS system assisting a two-way P2P communication link, as shown in Fig. 1. In particular, each user equipment (UE) operates in FD mode and therefore is equipped with either a single shared-antenna or a pair of separate antennas for signal transmission and reception, depending on the FD implementation [7]. In addition, $\mathcal{N} = \{1, \dots, N\}$ represents the set of available locations for installing an IRS (with $N \geq 1$), while $\mathcal{I} = \{i_1, \dots, i_I\} \subseteq \mathcal{N}$ (where $I = |\mathcal{I}|$) stands for the set of finally installed IRSs. In each time-slot, we assume that exactly one IRS from the set \mathcal{I} is active and the remaining IRSs are idle (i.e., non-reflective). UE-1 transmits its data to UE-2, through the active

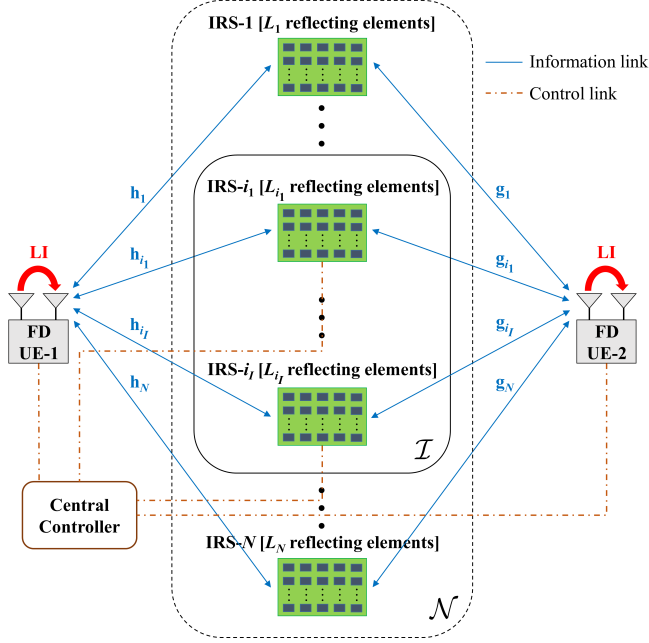


Fig. 1. Multi-IRS system assisting two-way FD communication with reciprocal channels and negligible direct link. The set of available IRS locations, \mathcal{N} , and the set of finally installed IRSs, \mathcal{I} , are illustrated by the dashed-outline and solid-outline rectangles, respectively. In each time-slot, the central controller activates only one IRS from the set \mathcal{I} , while the remaining IRSs are idle (i.e., non-reflective).

IRS, and UE-2 transmits its data to UE-1, through the same IRS, simultaneously (i.e., within the same time-slot) by using the same frequency band. The transmit power of each UE is considered *fixed* for all time-slots; power control is outside the scope of this paper. Since both UEs suffer from strong loop-interference (LI) due to the FD operation, they employ the same LI-cancellation techniques (e.g., passive and active suppression in the analog/digital domain [7]–[9]), resulting in residual LI.

Moreover, the total UE-to-IRS and IRS-to-UE transmission time is within a coherence interval of the wireless channel. As a result, the forward and backward channels between a UE and an IRS can be regarded almost identical (*reciprocal channels*) [11]. Also, the direct link between UEs is considered strongly attenuated (high path-loss) due to the long distance, high carrier-frequency, or severe blockage by physical obstacles (*no direct link*). All IRSs are assumed to be passive (i.e., performing only phase shifts without amplification) and they have negligible delay regarding the reflection of incident electromagnetic waves. We assume *perfect channel state information (CSI)*, i.e., without estimation errors, and *global CSI knowledge*, i.e., available to both UEs. Furthermore, there is a *central controller* that performs the IRS activation, adjusts the IRS phase-shifts and communicates the necessary CSI knowledge between UEs via separate low-latency wireless/wired backhaul links (illustrated by dash-dotted lines in Fig. 1).

Let L_n be the number of reflecting elements of the n^{th} IRS. The channel coefficient from UE-1 (UE-2) to the ℓ^{th} reflecting element of the n^{th} IRS is denoted by $h_{n,\ell} = |h_{n,\ell}| e^{j\vartheta_{n,\ell}}$

(respectively, $g_{n,\ell} = |g_{n,\ell}| e^{j\psi_{n,\ell}}$), for every $n \in \mathcal{N}$ and $\ell \in \mathcal{L}_n = \{1, \dots, L_n\}$. For notational convenience, the channel coefficients corresponding to the n^{th} IRS can be grouped in vector form, i.e., $\mathbf{h}_n = [h_{n,1}, \dots, h_{n,L_n}]^T$ and $\mathbf{g}_n = [g_{n,1}, \dots, g_{n,L_n}]^T$. All channel coefficients are assumed to be *independent and identically distributed (i.i.d.)*¹ complex normal/Gaussian random variables with zero mean and variance σ^2 , therefore, $|h_{n,\ell}|, |g_{n,\ell}| \sim \text{Rayleigh}(\sigma/\sqrt{2})$. Also, the channel coefficients are considered constant within any time-slot. The diagonal ($L_n \times L_n$) phase-shift matrix of the n^{th} IRS is given by $\Phi_n = \text{diag}(e^{j\phi_{n,1}}, \dots, e^{j\phi_{n,L_n}})$, i.e., we consider only phase-shifts and not amplitude attenuation.

Under the above assumptions and following a similar approach with [11], the received signals at UE-1 and UE-2 in time-slot t (after the LI mitigation), when only the n^{th} IRS is active, are expressed as follows

$$y_1(t) = \sqrt{P_2} \sqrt{\delta_{n,2} \delta_{n,1}} \mathbf{g}_n^T \Phi_n \mathbf{h}_n s_2(t) + \sqrt{P_1} \delta_{n,1} \mathbf{h}_n^T \Phi_n \mathbf{h}_n s_1(t) + \xi_1(t) + w_1(t), \quad (1)$$

$$y_2(t) = \sqrt{P_1} \sqrt{\delta_{n,1} \delta_{n,2}} \mathbf{h}_n^T \Phi_n \mathbf{g}_n s_1(t) + \sqrt{P_2} \delta_{n,2} \mathbf{g}_n^T \Phi_n \mathbf{g}_n s_2(t) + \xi_2(t) + w_2(t), \quad (2)$$

where P_k , $s_k(t)$, $\xi_k(t)$ and $w_k(t)$ are the transmit power, information symbol, residual LI and additive white Gaussian noise (AWGN) of UE- k , respectively, for $k \in \{1, 2\}$. In addition, $\delta_{n,k} = A_0 d_{n,k}^{-\alpha}$ accounts for the large-scale path loss between the n^{th} IRS and UE- k , where A_0 is a positive constant that depends on the carrier frequency, $d_{n,k}$ is their Euclidean distance, and α is the path-loss exponent which depends on the wireless propagation environment. Note that, in the above equations, the first term represents the desired signal, while the second term is the self-interference (SI) induced by the IRS reflection of users' own transmitted symbols. Given that UE- k has knowledge of P_k , $s_k(t)$, $\delta_{n,k}$, \mathbf{h}_n (required for $k = 1$), \mathbf{g}_n (needed for $k = 2$), and Φ_n , it can completely remove the SI. Moreover, the residual LI $\xi_k(t)$ and AWGN $w_k(t)$ are modeled as independent zero-mean complex Gaussian random variables with variances $\sigma_{\text{LI}_k}^2$ and $\sigma_{w_k}^2$, respectively. The variance of $\xi_k(t)$ can be further expressed as $\sigma_{\text{LI}_k}^2 = \omega P_k^\nu$, where the constants $\omega > 0$ and $\nu \in [0, 1]$ depend on the LI cancellation technique applied at the UEs [11].

For the sake of simplicity, we assume the following: $P_1 = P_2 = P$ (the same transmit power), $\mathbb{E}(|s_1(t)|^2) = \mathbb{E}(|s_2(t)|^2) = 1$ (unit-power information symbols), $\sigma_{w_1}^2 = \sigma_{w_2}^2 = \sigma_w^2$ and $\sigma_{\text{LI}_1}^2 = \sigma_{\text{LI}_2}^2 = \sigma_{\text{LI}}^2 (= \omega P^\nu)$ (equal noise and residual-LI power). Consequently, the *instantaneous* signal-to-interference-plus-noise ratio (SINR) at both UEs, after the SI elimination, when communicating via the n^{th} IRS is given by²

$$\gamma_n = \rho_n \left| \sum_{\ell \in \mathcal{L}_n} |h_{n,\ell}| |g_{n,\ell}| e^{j(\phi_{n,\ell} + \vartheta_{n,\ell} + \psi_{n,\ell})} \right|^2, \quad (3)$$

¹This can be achieved if the distances between the reflecting elements are large enough.

²In order to derive the SINR formula, observe that $\mathbf{g}_n^T \Phi_n \mathbf{h}_n = (\mathbf{g}_n^T \Phi_n \mathbf{h}_n)^T = \mathbf{h}_n^T \Phi_n \mathbf{g}_n = \sum_{\ell \in \mathcal{L}_n} h_{n,\ell} e^{j\phi_{n,\ell}} g_{n,\ell} = \sum_{\ell \in \mathcal{L}_n} |h_{n,\ell}| |g_{n,\ell}| e^{j(\phi_{n,\ell} + \vartheta_{n,\ell} + \psi_{n,\ell})}$.

where

$$\rho_n = \frac{P\delta_n}{\sigma_{\text{LI}}^2 + \sigma_w^2}, \quad (4)$$

with $\delta_n = \delta_{n,1}\delta_{n,2}$ being the overall path-loss between the two UEs through the n^{th} IRS. This SINR formula is quite similar to that in [11], except for the total path-loss term δ_n . Herein, however, we study a generalization of the system configuration presented in [11], including multiple IRSs and exploiting their geometric characteristics.

Furthermore, the IRS phase-shifts are optimally designed in order to maximize the instantaneous SINR, that is,

$$\phi_{n,\ell}^* = -\vartheta_{n,\ell} - \psi_{n,\ell}, \quad \forall \ell \in \mathcal{L}_n = \{1, \dots, L_n\}. \quad (5)$$

Note that the IRS phase-shifts are adjusted by the central controller after obtaining the necessary CSI knowledge (channel coefficients' phases) from the UE that performs the channel estimation. Also, we assume IRS phase-shifts *without quantization errors*, i.e., the IRS phase-shift resolution is infinite; in practice, if the number of bits, B , used for controlling the phase of a reflecting element is very large (resulting in 2^B possible discrete values), then the quantization error can be considered insignificant.

Therefore, the maximum SINR at both UEs (when communicating via the n^{th} IRS) is written as follows

$$\gamma_n^* = \rho_n \left(\sum_{\ell \in \mathcal{L}_n} |h_{n,\ell}| |g_{n,\ell}| \right)^2 = \rho_n \zeta_n^2, \quad (6)$$

where $\zeta_n = \sum_{\ell \in \mathcal{L}_n} \zeta_{n,\ell}$, with $\zeta_{n,\ell} = |h_{n,\ell}| |g_{n,\ell}| \geq 0$, $\forall \ell \in \mathcal{L}_n$. Observe that the Rayleigh-product random variables $\{\zeta_{n,\ell}\}_{\ell \in \mathcal{L}_n}$ are i.i.d. and, according to [11], the cumulative distribution function (CDF) of each one can be expressed as

$$F(u) \triangleq \Pr(\zeta_{n,\ell} \leq u) = 1 - \frac{2u}{\sigma^2} K_1 \left(\frac{2u}{\sigma^2} \right), \quad \forall u \geq 0, \quad (7)$$

where $K_1(\cdot)$ is the modified Bessel function of the second kind of the first order.

In addition, given an SINR threshold γ_{th} , the outage probability of each UE, defined as $P_{\text{out},n}(L_n) \triangleq \Pr(\gamma_n^* \leq \gamma_{\text{th}}) = \Pr(\zeta_n \leq \sqrt{\gamma_{\text{th}}/\rho_n})$, can be approximated by the CDF of the Gamma distribution [11], i.e.,

$$P_{\text{out},n}(L_n) \approx \frac{1}{\Gamma(\tau L_n)} \gamma \left(\tau L_n, \frac{1}{v} \sqrt{\frac{\gamma_{\text{th}}}{\rho_n}} \right) \triangleq \tilde{P}_{\text{out},n}(L_n), \quad (8)$$

where $\Gamma(\cdot)$ is the gamma function, $\gamma(\cdot, \cdot)$ is the lower incomplete gamma function, $\tau = \pi^2/(16 - \pi^2)$ and $v = (16 - \pi^2)\sigma^2/4\pi$. Although the Gamma approximation of outage probability is very useful for performance analysis, it is not versatile/flexible enough for optimization purposes, since it contains the number of reflecting elements, L_n , inside both gamma functions.

Nevertheless, in order to achieve mathematical tractability, we can construct an upper bound of outage probability as follows

$$\begin{aligned} P_{\text{out},n}(L_n) &= \Pr \left(\sum_{\ell \in \mathcal{L}_n} \zeta_{n,\ell} \leq \sqrt{\gamma_{\text{th}}/\rho_n} \right) \\ &\stackrel{(a)}{\leq} \Pr \left(\max_{\ell \in \mathcal{L}_n} \{\zeta_{n,\ell}\} \leq \sqrt{\gamma_{\text{th}}/\rho_n} \right) \\ &= \Pr \left(\bigcap_{\ell \in \mathcal{L}_n} \{\zeta_{n,\ell} \leq \sqrt{\gamma_{\text{th}}/\rho_n}\} \right) \\ &\stackrel{(b)}{=} \prod_{\ell \in \mathcal{L}_n} \Pr(\zeta_{n,\ell} \leq \sqrt{\gamma_{\text{th}}/\rho_n}) \\ &\stackrel{(c)}{=} \left[F(\sqrt{\gamma_{\text{th}}/\rho_n}) \right]^{L_n} \triangleq \bar{P}_{\text{out},n}(L_n), \end{aligned} \quad (9)$$

where inequality (a) is due to the fact that $\sum_{\ell \in \mathcal{L}_n} \zeta_{n,\ell} \geq \max_{\ell \in \mathcal{L}_n} \{\zeta_{n,\ell}\}$, while equalities (b) and (c) follows from the independence of random variables $\{\zeta_{n,\ell}\}_{\ell \in \mathcal{L}_n}$ and equation (7), respectively. It is interesting to observe that $P_{\text{out},n}(L_n)$ and $\bar{P}_{\text{out},n}(L_n)$ are *nonincreasing functions of L_n* . In addition, $\lim_{L_n \rightarrow \infty} P_{\text{out},n}(L_n) = \lim_{L_n \rightarrow \infty} \bar{P}_{\text{out},n}(L_n) = 0$, provided that $F(\sqrt{\gamma_{\text{th}}/\rho_n}) < 1$. At this point, we would like to emphasize that the upper bound is not very tight in general. However, from the optimization perspective (with respect to L_n), this upper bound has the same monotonicity as the exact outage probability and is also suitable for constructing relaxation problems that are solvable in polynomial time (see Section IV-B). In other words, it achieves a reasonable compromise between accuracy/tightness and optimization tractability.

A. IRS Activation Policy

As we mentioned earlier, exactly one IRS is activated in each time-slot by the central controller, while the remaining IRSs are inactive (i.e., non-reflective). The activation of multiple IRSs within the same time-slot would cause inter-IRS reflections of the transmitted signal (i.e., between the active IRSs), which complicates the system analysis and is beyond the scope of this paper.

In particular, the central controller activates the IRS that achieves the maximum (instantaneous) SINR at UEs among the installed IRSs, that is,

$$i^* \in \arg \max_{i \in \mathcal{I}} \{\gamma_i^*\} \Leftrightarrow \gamma_{i^*}^* = \max_{i \in \mathcal{I}} \{\gamma_i^*\}, \quad (10)$$

where γ_i^* is given by (6).

B. Upper Bound of System Outage Probability

Based on the aforementioned IRS activation strategy, the *system outage probability* can be computed as follows

$$\begin{aligned} P_{\text{out}}(\mathcal{I}, \mathbf{L}) &\triangleq \Pr(\gamma_{i^*}^* \leq \gamma_{\text{th}}) \stackrel{(d)}{=} \Pr \left(\max_{i \in \mathcal{I}} \{\gamma_i^*\} \leq \gamma_{\text{th}} \right) \\ &= \Pr \left(\bigcap_{i \in \mathcal{I}} \{\gamma_i^* \leq \gamma_{\text{th}}\} \right) \stackrel{(e)}{=} \prod_{i \in \mathcal{I}} \Pr(\gamma_i^* \leq \gamma_{\text{th}}) \\ &\stackrel{(f)}{=} \prod_{i \in \mathcal{I}} P_{\text{out},i}(L_i), \end{aligned} \quad (11)$$

where $\mathbf{L} = [L_1, \dots, L_N]^\top$ and γ_{th} is the SINR threshold. Equalities (d), (e) and (f) follow from (10), the independence of $\{\gamma_i^*\}_{i \in \mathcal{I}}$ (due to the independence of $\{\zeta_i\}_{i \in \mathcal{I}}$) and the definition of $P_{\text{out},i}(L_i) \triangleq \Pr(\gamma_i^* \leq \gamma_{\text{th}})$, respectively.

Afterwards, by combining (11) with (9), we obtain the following upper bound of system outage probability

$$P_{\text{out}}(\mathcal{I}, \mathbf{L}) \leq \prod_{i \in \mathcal{I}} \left[F(\sqrt{\gamma_{\text{th}}/\rho_i}) \right]^{L_i} \triangleq \bar{P}_{\text{out}}(\mathcal{I}, \mathbf{L}). \quad (12)$$

C. IRS Installation Cost Model

In this paper, we model the installation cost of IRS $n \in \mathcal{N}$ as an *affine function* of the number of reflecting elements, i.e.,

$$C_n(L_n) = c_n + \lambda_n L_n, \quad (13)$$

where $c_n \geq 0$ is the fixed deployment cost and $\lambda_n \geq 0$ is the cost rate (measured in cost-units per element) of the corresponding IRS. In addition, the total installation cost is defined as the sum of the costs of all IRSs in the set \mathcal{I} , i.e.,

$$C_{\text{tot}}(\mathcal{I}, \mathbf{L}) = \sum_{i \in \mathcal{I}} C_i(L_i) = \sum_{i \in \mathcal{I}} (c_i + \lambda_i L_i). \quad (14)$$

Remark 1: In general, the IRS installation cost can be any nondecreasing function of the number of reflecting elements. In this case, we can approximate the installation cost by an affine function given by (13). In particular, the coefficients $\{c_n, \lambda_n\}$ can be adjusted so as to minimize the error between the two functions (a procedure known as *curve fitting*) within a given interval of interest, e.g., for $L_n \in \{L_n^{\min}, \dots, L_n^{\max}\}$.

D. Half-Duplex (HD) Scheme

If the system operates in half-duplex (HD) mode, then the UEs transmit their data in two distinct time-slots: time-slot 1 is allocated for UE-1 transmission and time-slot 2 for UE-2 transmission. As a result, each UE is equipped with a single antenna, utilizes the same frequency band, and there is no interference at all (neither self nor loop interference).

In this case, we can study the performance of HD scheme by appropriately modifying the previous equations of FD scheme. In particular, we should replace ρ_n in (4) with $\rho_n^{\text{HD}} = P\delta_n/\sigma_w^2$ (since $\sigma_{\text{LI}}^2 = 0$) and also γ_{th} with $\gamma_{\text{th}}^{\text{HD}} = (1 + \gamma_{\text{th}})^2 - 1$, which is obtained by equating the spectral efficiencies of the two schemes, i.e., $\log(1 + \gamma_{\text{th}}) = \frac{1}{2} \log(1 + \gamma_{\text{th}}^{\text{HD}})$. The latter replacement is made for fair comparison between FD and HD scenarios in terms of outage probability.

III. OPTIMIZATION PROBLEM FORMULATION AND COMPUTATIONAL COMPLEXITY

In this section, we study the minimization of system outage probability under various constraints. More precisely, we minimize the upper bound $\bar{P}_{\text{out}}(\mathcal{I}, \mathbf{L})$ given by (12) instead of the exact system outage probability or its gamma approximation; this is done for *mathematical tractability when constructing a relaxation problem* (see Section IV-B). In addition, the IRS deployment problem consists of two components, namely, the

selection of locations for installing IRSs and the determination of IRS sizes (that is, the number of reflecting elements).

Herein, we consider a *predetermined* and *finite* set of available IRS locations, thus taking into account physical constraints for the IRS positions. This is of great practical interest, since IRSs are usually installed on the facades, walls or ceilings of existing buildings. However, if we are interested in installing IRSs within a bounded continuous area, then this region can be divided into a sufficiently large finite number of distinct points (this technique is known as discretization). As a result, the proposed approach is still applicable.

As reported in Section II, the IRSs in the set \mathcal{I} are installed only once, during the initial design of the system. After the installation phase, the central controller performs, in each time-slot, the IRS activation between the installed IRSs.

In this context, the *joint IRS location and size optimization* problem is formulated as follows

$$\min_{\mathcal{I}, \mathbf{L}} \bar{P}_{\text{out}}(\mathcal{I}, \mathbf{L}) \triangleq \prod_{i \in \mathcal{I}} \left[F(\sqrt{\gamma_{\text{th}}/\rho_i}) \right]^{L_i} \quad (15a)$$

$$\text{s.t. } \mathcal{I} \subseteq \mathcal{N} \quad (15b)$$

$$L_n \in \{L_n^{\min}, \dots, L_n^{\max}\}, \quad \forall n \in \mathcal{N} \quad (15c)$$

$$|\mathcal{I}| \leq M \quad (15d)$$

$$L_{\text{tot}}(\mathcal{I}, \mathbf{L}) \triangleq \sum_{i \in \mathcal{I}} L_i \leq L_{\text{tot}}^{\max} \quad (15e)$$

$$C_{\text{tot}}(\mathcal{I}, \mathbf{L}) \triangleq \sum_{i \in \mathcal{I}} (c_i + \lambda_i L_i) \leq C_{\text{tot}}^{\max}, \quad (15f)$$

where $L_n^{\min}, L_n^{\max} \geq 0$ are the minimum and maximum number of reflecting elements of the n^{th} IRS, respectively (with $L_n^{\min} \leq L_n^{\max}$). For example, in a specific location/building there are some limitations on the area (dimensions) that an IRS can occupy. Also, $M \in \{0, 1, \dots, N\}$ is the maximum number of installed IRSs, resulting in an *IRS-cardinality constraint*. Finally, $L_{\text{tot}}^{\max}, C_{\text{tot}}^{\max} \geq 0$ denote the maximum total number of reflecting elements and the maximum total IRS installation cost, respectively. Note that constraint (15e) implicitly imposes an upper bound on the *overall signaling overhead* (channel estimation and feedback), which is required for IRS activation and phase adjustments. In addition, for a given $\mathcal{I} \subseteq \mathcal{N}$, the values of $\{L_n\}_{n \in \mathcal{N} \setminus \mathcal{I}}$ are ultimately meaningless, since no IRS is installed at these locations.

A. Transformation into Discrete Optimization Problem

Now, let us introduce a vector of binary (0/1) variables $\mathbf{x} = [x_1, \dots, x_N]^\top$ such that, for all $n \in \mathcal{N}$, $x_n = 1$ if and only if (iff) $n \in \mathcal{I}$. Subsequently, the set \mathcal{I} is replaced by the vector \mathbf{x} in all functions that contained it with a slight abuse of notation. In particular, \mathcal{I} and \mathbf{x} are interchangeable because the one can be derived from the other by exploiting their iff-relation. With these in mind, we can make the following observations:³ 1) $\bar{P}_{\text{out}}(\mathcal{I}, \mathbf{L}) = \prod_{n \in \mathcal{N}} \left[F(\sqrt{\gamma_{\text{th}}/\rho_n}) \right]^{x_n L_n}$, 2) $|\mathcal{I}| = \sum_{n \in \mathcal{N}} x_n$, 3) $L_{\text{tot}}(\mathcal{I}, \mathbf{L}) = \sum_{n \in \mathcal{N}} x_n L_n$ and 4)

³In order to avoid the undefined quantity 0^0 , we assume that $P_{\text{out},n}(L_n) > 0$, which implies $\left[F(\sqrt{\gamma_{\text{th}}/\rho_n}) \right]^{L_n} > 0$, for all $n \in \mathcal{N}$.

$C_{\text{tot}}(\mathcal{I}, \mathbf{L}) = \sum_{n \in \mathcal{N}} (c_n + \lambda_n L_n) x_n$. Therefore, problem (15) can be written as follows

$$\min_{\mathbf{x}, \mathbf{L}} \bar{P}_{\text{out}}(\mathbf{x}, \mathbf{L}) \triangleq \prod_{n \in \mathcal{N}} \left[F(\sqrt{\gamma_{\text{th}}/\rho_n}) \right]^{x_n L_n} \quad (16a)$$

$$\text{s.t. } x_n \in \{0, 1\}, \quad \forall n \in \mathcal{N} \quad (16b)$$

$$L_n \in \{L_n^{\min}, \dots, L_n^{\max}\}, \quad \forall n \in \mathcal{N} \quad (16c)$$

$$\sum_{n \in \mathcal{N}} x_n \leq M \quad (16d)$$

$$L_{\text{tot}}(\mathbf{x}, \mathbf{L}) \triangleq \sum_{n \in \mathcal{N}} x_n L_n \leq L_{\text{tot}}^{\max} \quad (16e)$$

$$C_{\text{tot}}(\mathbf{x}, \mathbf{L}) \triangleq \sum_{n \in \mathcal{N}} (c_n + \lambda_n L_n) x_n \leq C_{\text{tot}}^{\max}, \quad (16f)$$

where \mathbf{x}, \mathbf{L} are the decision/optimization variables.

Since $\log(\cdot)$ is a monotonically increasing function, we can replace $\bar{P}_{\text{out}}(\mathbf{x}, \mathbf{L})$ with its logarithm, without altering the set of optimal solutions. Hence, we obtain the equivalent *discrete optimization problem*

$$\min_{\mathbf{x}, \mathbf{L}} G(\mathbf{x}, \mathbf{L}) \triangleq \log(\bar{P}_{\text{out}}(\mathbf{x}, \mathbf{L})) = \sum_{n \in \mathcal{N}} \beta_n (x_n L_n) \quad (17a)$$

$$\text{s.t. } x_n \in \{0, 1\}, \quad \forall n \in \mathcal{N} \quad (17b)$$

$$L_n \in \{L_n^{\min}, \dots, L_n^{\max}\}, \quad \forall n \in \mathcal{N} \quad (17c)$$

$$\sum_{n \in \mathcal{N}} x_n \leq M \quad (17d)$$

$$\sum_{n \in \mathcal{N}} x_n L_n \leq L_{\text{tot}}^{\max} \quad (17e)$$

$$\sum_{n \in \mathcal{N}} c_n x_n + \sum_{n \in \mathcal{N}} \lambda_n (x_n L_n) \leq C_{\text{tot}}^{\max}, \quad (17f)$$

where $\beta_n = \log\left(F(\sqrt{\gamma_{\text{th}}/\rho_n})\right) \leq 0$ for all $n \in \mathcal{N}$. Throughout the paper, $(\mathbf{x}^*, \mathbf{L}^*)$ and $G^* = G(\mathbf{x}^*, \mathbf{L}^*)$ denote an optimal solution and the global minimum of problem (17), respectively. As we will see later, this problem is rather unlikely to be globally solved in polynomial time due to its discrete (and, thus, nonconvex) structure.

Remark 2 (Feasibility): Optimization problem (17) is *always* feasible, since the solution $(\mathbf{x}, \mathbf{L}) = (\mathbf{0}_N, \mathbf{L}^{\min})$, where $\mathbf{L}^{\min} = [L_1^{\min}, \dots, L_N^{\min}]^\top$, satisfies all constraints.

B. NP-Hardness

Afterwards, we examine the computational complexity of finding a (globally) optimal solution to problem (17).

Theorem 1 (NP-hardness): The discrete optimization problem (17) is NP-hard.

Proof: It is sufficient to show that there is a special case of problem (17) which is NP-hard. Let us consider the following case: $L_n^{\min} = L_n^{\max} = L_n^\circ > 0$ (hence, $L_n = L_n^\circ$ for all $n \in \mathcal{N}$, $M = N$ (so, the IRS-cardinality constraint can be omitted, because $\sum_{n \in \mathcal{N}} x_n \leq N$ for all $\mathbf{x} \in \{0, 1\}^N$) and $L_{\text{tot}}^{\max} = \sum_{n \in \mathcal{N}} L_n^{\max}$ (therefore, the constraint of maximum total number of reflecting elements can be omitted, since $\sum_{n \in \mathcal{N}} x_n L_n \leq \sum_{n \in \mathcal{N}} L_n \leq \sum_{n \in \mathcal{N}} L_n^{\max}$

for all $\mathbf{x} \in \{0, 1\}^N$ and $\mathbf{L} \in \times_{n \in \mathcal{N}} \{L_n^{\min}, \dots, L_n^{\max}\}$). As a consequence, problem (17) reduces to

$$\min_{\mathbf{x}} \sum_{n \in \mathcal{N}} (\beta_n L_n^\circ) x_n \quad (18a)$$

$$\text{s.t. } x_n \in \{0, 1\}, \quad \forall n \in \mathcal{N} \quad (18b)$$

$$\sum_{n \in \mathcal{N}} (c_n + \lambda_n L_n^\circ) x_n \leq C_{\text{tot}}^{\max}. \quad (18c)$$

By converting it into a maximization problem, we obtain

$$\max_{\mathbf{x}} \sum_{n \in \mathcal{N}} \varphi_n x_n \quad (19a)$$

$$\text{s.t. } x_n \in \{0, 1\}, \quad \forall n \in \mathcal{N} \quad (19b)$$

$$\sum_{n \in \mathcal{N}} \theta_n x_n \leq C_{\text{tot}}^{\max}, \quad (19c)$$

where $\varphi_n = -\beta_n L_n^\circ \geq 0$ and $\theta_n = c_n + \lambda_n L_n^\circ$ for every $n \in \mathcal{N}$. A crucial observation here is that each coefficient in $\{\varphi_n, \theta_n\}_{n \in \mathcal{N}}$ can be *any* positive integer. To prove this, let $\kappa_n, \mu_n > 0$ be arbitrary integers. Then, we can find a problem instance such that $\rho_n = \gamma_{\text{th}} / (F^{-1}(e^{-\kappa_n/L_n^\circ}))^2$, $0 \leq c_n \leq \mu_n$ and $\lambda_n = (\mu_n - c_n)/L_n^\circ \geq 0$ for all $n \in \mathcal{N}$, where $F^{-1}(\cdot)$ is the inverse function of $F(\cdot)$ given by (7); the existence of $F^{-1}(\cdot)$ is guaranteed, because $F(\cdot)$ is continuous and monotonically increasing. As a result, $\beta_n = \log\left(F(\sqrt{\gamma_{\text{th}}/\rho_n})\right) = -\kappa_n/L_n^\circ < 0$, thus $\varphi_n = \kappa_n$, and $\theta_n = \mu_n$ as well.

Furthermore, if $\{\varphi_n, \theta_n\}_{n \in \mathcal{N}}$ and C_{tot}^{\max} are all restricted to be positive integers, then problem (19) becomes identical to the *knapsack problem* which is known to be NP-hard [29]; this completes the proof. \square

Remark 3: Even if we consider the exact formula $P_{\text{out}}(\mathbf{x}, \mathbf{L}) \triangleq \prod_{n \in \mathcal{N}} [P_{\text{out},n}(L_n)]^{x_n}$ or the gamma approximation $\tilde{P}_{\text{out}}(\mathbf{x}, \mathbf{L}) \triangleq \prod_{n \in \mathcal{N}} [\tilde{P}_{\text{out},n}(L_n)]^{x_n}$ as the objective function in (17), the new optimization problems are still NP-hard. This can be easily proved by following similar arguments as above and replacing the objective coefficients φ_n in problem (19) with $\varphi'_n = -\log(P_{\text{out},n}(L_n^\circ))$ or $\varphi''_n = -\log(\tilde{P}_{\text{out},n}(L_n^\circ))$, respectively.

IV. OPTIMIZATION ALGORITHMS

Subsequently, we present the exhaustive-search (or brute-force) technique, a linear-programming relaxation (LPR), a greedy method as well as a randomized algorithm with complexity analysis for each one. The solution of LPR plays a central role in the design of greedy and randomized algorithms.

A. Exhaustive-Enumeration Algorithm

The exhaustive-enumeration method checks all possible solutions and selects that with the minimum objective value satisfying all constraints. In particular, for all subsets \mathcal{I} of \mathcal{N} with cardinality at most M , the algorithm examines all arrangements of reflecting elements. More specifically, for a given subset \mathcal{I} , the number of arrangements of reflecting elements is $\prod_{i \in \mathcal{I}} (L_i^{\max} - L_i^{\min} + 1)$, because the decision variable L_i can take $(L_i^{\max} - L_i^{\min} + 1)$ distinct values. In addition, for each

arrangement, the algorithm requires $\Theta(|\mathcal{I}|)$ time to compute the objective value, $G(\mathcal{I}, \mathbf{L}) = \sum_{i \in \mathcal{I}} \beta_i L_i$, and check the feasibility of constraints $L_{\text{tot}}(\mathcal{I}, \mathbf{L}) \leq L_{\text{tot}}^{\max}$, $C_{\text{tot}}(\mathcal{I}, \mathbf{L}) \leq C_{\text{tot}}^{\max}$. Therefore, its overall runtime is $\Theta\left(\sum_{\substack{\mathcal{I} \subseteq \mathcal{N} \\ |\mathcal{I}| \leq M}} |\mathcal{I}| \prod_{i \in \mathcal{I}} R_i\right)$, where $R_n = L_n^{\max} - L_n^{\min} + 1$ for all $n \in \mathcal{N}$.

It is not difficult to conclude that the algorithm has *exponential complexity* in terms of the size of the problem. Let us suppose that $R_n = R \geq 1$ for all $n \in \mathcal{N}$. In this case, the algorithm requires $\Theta\left(\sum_{\substack{\mathcal{I} \subseteq \mathcal{N} \\ |\mathcal{I}| \leq M}} |\mathcal{I}| R^{|\mathcal{I}|}\right) = \Omega\left(\sum_{\substack{\mathcal{I} \subseteq \mathcal{N} \\ |\mathcal{I}|=M}} |\mathcal{I}| R^{|\mathcal{I}|}\right) = \Omega\left(\binom{N}{M} M R^M\right)$ arithmetic operations to find the global minimum. Furthermore, if $M = \lceil N/2 \rceil$, then its complexity becomes $\Omega\left(2^N \sqrt{N} R^{N/2}\right)$, since $\binom{N}{\lceil N/2 \rceil} = \Theta\left(\frac{2^N}{\sqrt{N}}\right)$ and $\lceil N/2 \rceil \geq N/2$.

Ultimately, albeit achieving a globally optimal solution, the exhaustive-enumeration algorithm has extremely high complexity and is therefore impractical.

B. Lower Bound Using Linear-Programming Relaxation

Despite the difficulty of computing the global minimum, we will show how to efficiently compute (in polynomial-time) a lower bound of the optimum value G^* . Firstly, by using auxiliary decision variables $\mathbf{z} = [z_1, \dots, z_N]^T$, problem (17) can be equivalently written in the following form

$$\min_{\mathbf{x}, \mathbf{L}, \mathbf{z}} \sum_{n \in \mathcal{N}} \beta_n z_n \quad (20a)$$

$$\text{s.t. } x_n \in \{0, 1\}, \quad \forall n \in \mathcal{N} \quad (20b)$$

$$L_n \in \{L_n^{\min}, \dots, L_n^{\max}\}, \quad \forall n \in \mathcal{N} \quad (20c)$$

$$z_n = x_n L_n, \quad \forall n \in \mathcal{N} \quad (20d)$$

$$\sum_{n \in \mathcal{N}} x_n \leq M \quad (20e)$$

$$\sum_{n \in \mathcal{N}} z_n \leq L_{\text{tot}}^{\max} \quad (20f)$$

$$\sum_{n \in \mathcal{N}} c_n x_n + \sum_{n \in \mathcal{N}} \lambda_n z_n \leq C_{\text{tot}}^{\max}. \quad (20g)$$

Secondly, by relaxing the integer/discrete constraints, $x_n \in \{0, 1\}$ and $L_n \in \{L_n^{\min}, \dots, L_n^{\max}\}$, we have

$$\min_{\mathbf{x}, \mathbf{L}, \mathbf{z}} \sum_{n \in \mathcal{N}} \beta_n z_n \quad (21a)$$

$$\text{s.t. } 0 \leq x_n \leq 1, \quad \forall n \in \mathcal{N} \quad (21b)$$

$$L_n^{\min} \leq L_n \leq L_n^{\max}, \quad \forall n \in \mathcal{N} \quad (21c)$$

$$z_n = x_n L_n, \quad \forall n \in \mathcal{N} \quad (21d)$$

$$\sum_{n \in \mathcal{N}} x_n \leq M \quad (21e)$$

$$\sum_{n \in \mathcal{N}} z_n \leq L_{\text{tot}}^{\max} \quad (21f)$$

$$\sum_{n \in \mathcal{N}} c_n x_n + \sum_{n \in \mathcal{N}} \lambda_n z_n \leq C_{\text{tot}}^{\max}. \quad (21g)$$

Notice that this problem is nonlinear due to the equality constraints $z_n = x_n L_n$. In order to obtain a linear problem,

we apply further relaxation by replacing the set of constraints $L_n^{\min} \leq L_n \leq L_n^{\max}$ and $z_n = x_n L_n$ with the linear constraints $L_n^{\min} x_n \leq z_n \leq L_n^{\max} x_n$. In this way, we can remove the decision variable \mathbf{L} and formulate the following *linear-programming relaxation (LPR)* problem

$$\min_{\mathbf{x}, \mathbf{z}} \sum_{n \in \mathcal{N}} \beta_n z_n \quad (22a)$$

$$\text{s.t. } 0 \leq x_n \leq 1, \quad \forall n \in \mathcal{N} \quad (22b)$$

$$L_n^{\min} x_n \leq z_n \leq L_n^{\max} x_n, \quad \forall n \in \mathcal{N} \quad (22c)$$

$$\sum_{n \in \mathcal{N}} x_n \leq M \quad (22d)$$

$$\sum_{n \in \mathcal{N}} z_n \leq L_{\text{tot}}^{\max} \quad (22e)$$

$$\sum_{n \in \mathcal{N}} c_n x_n + \sum_{n \in \mathcal{N}} \lambda_n z_n \leq C_{\text{tot}}^{\max}. \quad (22f)$$

Note that the guaranteed feasibility of problem (17) (see Remark 2) implies the feasibility of problems (20), (21) and (22). In what follows, $(\mathbf{x}^\dagger, \mathbf{z}^\dagger)$ and $G^\dagger = \sum_{n \in \mathcal{N}} \beta_n z_n^\dagger$ denote an optimal solution and the global minimum of the LPR problem (22), respectively. Obviously, $G^\dagger \leq G^*$, that is, G^\dagger is a lower bound of G^* .

Finally, given that the linear problem (22) has $V = 2N = \Theta(N)$ decision variables and $U = 4N + 3 = \Theta(N)$ constraints, a globally optimal solution can be computed in $O((U + V)^{1.5} V^2) = O(N^{3.5})$ time using an interior-point method [30].

C. Deterministic Greedy Algorithm

Now, we are ready to develop a heuristic algorithm of polynomial complexity to obtain a feasible solution for the discrete problem (17). This procedure is given in Algorithm 1 and is called *LPR-based greedy algorithm (LPR-GA)*.

First, the proposed algorithm applies *deterministic rounding*, using the solution of LPR (step 1), in order to compute the decision variable \mathbf{L}' (steps 3–9):

$$L'_n = \begin{cases} \text{round}(z_n^\dagger/x_n^\dagger), & \text{if } x_n^\dagger \neq 0 \\ \text{round}\left(\frac{1}{2}(L_n^{\min} + L_n^{\max})\right), & \text{otherwise} \end{cases}, \quad \forall n \in \mathcal{N}. \quad (23)$$

Observe that, if $x_n^\dagger \neq 0$, then $L_n^{\min} \leq z_n^\dagger/x_n^\dagger \leq L_n^{\max}$ (due to the feasibility of LPR problem) and therefore $\text{round}(z_n^\dagger/x_n^\dagger) \in \{L_n^{\min}, \dots, L_n^{\max}\}$. Also, the same holds for $\text{round}\left(\frac{1}{2}(L_n^{\min} + L_n^{\max})\right)$ in case of $x_n^\dagger = 0$. In other words, the above deterministic rounding guarantees that $L'_n \in \{L_n^{\min}, \dots, L_n^{\max}\}$ for all $n \in \mathcal{N}$.

Concerning the computation of \mathbf{x}' , the proposed algorithm sorts the entries of $\mathbf{x}^\dagger = [x_1^\dagger, \dots, x_N^\dagger]^T \in [0, 1]^N$ in descending order (step 11). Then, by starting from the zero vector, it successively selects IRS locations (based on their sorting) until the violation of at least one of the constraints: $\sum_{n \in \mathcal{N}} x_n \leq M$, $L_{\text{tot}}(\mathbf{x}, \mathbf{L}) \leq L_{\text{tot}}^{\max}$ and $C_{\text{tot}}(\mathbf{x}, \mathbf{L}) \leq C_{\text{tot}}^{\max}$ (steps 12–17). Finally, it removes the last selected IRS location if $L_{\text{tot}} > L_{\text{tot}}^{\max}$ or $C_{\text{tot}} > C_{\text{tot}}^{\max}$ (steps 18–20); note that the IRS-cardinality constraint is automatically satisfied due to the construction of the while-loop, so there is no need to check it in step 18.

Algorithm 1 LPR-based Greedy Algorithm (LPR-GA)

Input: $N, \beta = [\beta_1, \dots, \beta_N]^\top, \mathbf{L}^{\min} = [L_1^{\min}, \dots, L_N^{\min}]^\top,$
 $\mathbf{L}^{\max} = [L_1^{\max}, \dots, L_N^{\max}]^\top, M, L_{\text{tot}}^{\max}, \mathbf{c} = [c_1, \dots, c_N]^\top,$
 $\lambda = [\lambda_1, \dots, \lambda_N]^\top, C_{\text{tot}}^{\max}$

Output: A feasible solution $(\mathbf{x}', \mathbf{L}')$ of discrete problem (17)

- 1: Solve the LPR problem (22) to obtain an optimal solution $(\mathbf{x}^\dagger, \mathbf{z}^\dagger)$.
- 2: \triangleright *Computation of $\mathbf{L}' = [L'_1, \dots, L'_N]^\top$*
- 3: **for all** $n \in \mathcal{N}$ **do**
- 4: **if** $x_n^\dagger \neq 0$ **then**
- 5: $L'_n := \text{round}(z_n^\dagger/x_n^\dagger)$
- 6: **else**
- 7: $L'_n := \text{round}(\frac{1}{2}(L_n^{\min} + L_n^{\max}))$
- 8: **end if**
- 9: **end for**
- 10: \triangleright *Computation of $\mathbf{x}' = [x'_1, \dots, x'_N]^\top$*
- 11: Sort the entries of \mathbf{x}^\dagger in descending order. Let $(\sigma_1, \dots, \sigma_N) \in \Sigma_N$ be their order after sorting, where Σ_N is the set of all permutations of \mathcal{N} , therefore $x_{\sigma_1}^\dagger \geq \dots \geq x_{\sigma_N}^\dagger$.
- 12: $m := 1, L_{\text{tot}} := 0, C_{\text{tot}} := 0, \mathbf{x}' := \mathbf{0}_N$
- 13: **while** $(m \leq M) \wedge (L_{\text{tot}} \leq L_{\text{tot}}^{\max}) \wedge (C_{\text{tot}} \leq C_{\text{tot}}^{\max})$ **do**
- 14: $i := \sigma_m, x'_i := 1$
- 15: $L_{\text{tot}} := L_{\text{tot}} + L'_i, C_{\text{tot}} := C_{\text{tot}} + c_i + \lambda_i L'_i$
- 16: $m := m + 1$
- 17: **end while**
- 18: **if** $(L_{\text{tot}} > L_{\text{tot}}^{\max}) \vee (C_{\text{tot}} > C_{\text{tot}}^{\max})$ **then**
- 19: $x'_i := 0$
- 20: **end if**
- 21: **return** $(\mathbf{x}', \mathbf{L}')$

Obviously, the solution $(\mathbf{x}', \mathbf{L}')$ returned by Algorithm 1 is guaranteed to be feasible for problem (17), thus $G^* \leq G' \triangleq G(\mathbf{x}', \mathbf{L}')$, i.e., G' is an upper bound of G^* .

Remark 4 (A posteriori performance guarantee): It is possible to provide an approximation guarantee after the termination of Algorithm 1 using the already obtained solution of LPR, that is, $0 \leq G' - G^* \leq G' - G^\dagger$.

Regarding the complexity of Algorithm 1, the LPR problem can be solved in $O(N^{3.5})$ time, the computation of \mathbf{L}' requires $\Theta(N)$ time, while the computation of \mathbf{x}' requires $O(N \log N + N) = O(N \log N)$ arithmetic operations in total. Hence, the overall complexity of LPR-GA is $O(N^{3.5} + N + N \log N) = O(N^{3.5})$. In other words, it has the same asymptotic complexity (up to a constant) as the LPR problem.

D. Randomized Approximation Algorithm

Since problem (17) is NP-hard, a polynomial-time algorithm for computing its global optimum cannot exist, unless P=NP. However, we can use *randomized rounding*, a powerful technique, in order to achieve an *approximate solution with high probability*.

Afterwards, we present an efficient (i.e., polynomial-time) approximation algorithm that finds *provably near-optimal solutions*. This method is shown in Algorithm 2 and is referred

Algorithm 2 LPR-based Randomized Algorithm (LPR-RA)

Input: $N, \beta = [\beta_1, \dots, \beta_N]^\top, \mathbf{L}^{\min} = [L_1^{\min}, \dots, L_N^{\min}]^\top,$
 $\mathbf{L}^{\max} = [L_1^{\max}, \dots, L_N^{\max}]^\top, M, L_{\text{tot}}^{\max}, \mathbf{c} = [c_1, \dots, c_N]^\top,$
 $\lambda = [\lambda_1, \dots, \lambda_N]^\top, C_{\text{tot}}^{\max}$

Output: An approximate solution $(\tilde{\mathbf{x}}, \tilde{\mathbf{L}})$ of discrete problem (17)

- 1: Solve the LPR problem (22) to obtain an optimal solution $(\mathbf{x}^\dagger, \mathbf{z}^\dagger)$.
- 2: **for all** $n \in \mathcal{N}$ **do**
- 3: \triangleright *Computation of \tilde{x}_n*
- 4: $r := \text{rand}(0, 1)$
- 5: **if** $r \leq x_n^\dagger$ **then** \triangleright with probability x_n^\dagger
- 6: $\tilde{x}_n := 1$
- 7: **else** \triangleright with probability $1 - x_n^\dagger$
- 8: $\tilde{x}_n := 0$
- 9: **end if**
- 10: \triangleright *Computation of \tilde{L}_n*
- 11: **if** $x_n^\dagger \neq 0$ **then**
- 12: $s := \text{rand}(0, 1), L_n^\dagger := z_n^\dagger/x_n^\dagger$
- 13: **if** $s \leq \text{frac}(L_n^\dagger)$ **then** \triangleright with probability $\text{frac}(L_n^\dagger)$
- 14: $\tilde{L}_n := \lfloor L_n^\dagger \rfloor + 1$
- 15: **else** \triangleright with probability $1 - \text{frac}(L_n^\dagger)$
- 16: $\tilde{L}_n := \lfloor L_n^\dagger \rfloor$
- 17: **end if**
- 18: **else**
- 19: $\tilde{L}_n := \text{randi}(L_n^{\min}, L_n^{\max})$
- 20: **end if**
- 21: **end for**
- 22: **return** $(\tilde{\mathbf{x}}, \tilde{\mathbf{L}})$

to as *LPR-based randomized algorithm (LPR-RA)*.⁴

First of all, Algorithm 2 finds an optimal solution $(\mathbf{x}^\dagger, \mathbf{z}^\dagger)$ to the LPR problem in step 1, and then employs randomization (steps 2–21) to compute an approximate solution $(\tilde{\mathbf{x}}, \tilde{\mathbf{L}})$ according to the following probabilistic rules, for all $n \in \mathcal{N}$,

$$\tilde{x}_n = \begin{cases} 1, & \text{with probability } x_n^\dagger \\ 0, & \text{with probability } 1 - x_n^\dagger \end{cases} \quad (24)$$

and

$$\tilde{L}_n = \begin{cases} \lfloor L_n^\dagger \rfloor + 1, & \text{with probability } \text{frac}(L_n^\dagger) \\ \lfloor L_n^\dagger \rfloor, & \text{with probability } 1 - \text{frac}(L_n^\dagger) \end{cases}, \text{ if } x_n^\dagger \neq 0 \quad (25)$$

or

$$\tilde{L}_n \sim \text{Uniform}(\{L_n^{\min}, \dots, L_n^{\max}\}), \text{ if } x_n^\dagger = 0, \quad (26)$$

where $L_n^\dagger = z_n^\dagger/x_n^\dagger$ defined whenever $x_n^\dagger \neq 0$. For a given LPR solution $(\mathbf{x}^\dagger, \mathbf{z}^\dagger)$, the random variables $\{\tilde{x}_n, \tilde{L}_n\}_{n \in \mathcal{N}}$ are *independent*. Also, we define the random variable $\tilde{z}_n = \tilde{x}_n \tilde{L}_n$ for all $n \in \mathcal{N}$.

In case $x_n^\dagger \neq 0$, observe that $L_n^{\min} \leq L_n^\dagger \leq L_n^{\max}$ (because $L_n^{\min} x_n^\dagger \leq z_n^\dagger \leq L_n^{\max} x_n^\dagger$), therefore rule (25) implies that $\tilde{L}_n \in \{L_n^{\min}, \dots, L_n^{\max}\}$. Also, the same holds when $x_n^\dagger = 0$ due to (26). Hence, the probabilistic rules (24)–(26) ensure that the approximate solution returned by LPR-RA, $(\tilde{\mathbf{x}}, \tilde{\mathbf{L}})$, satisfies

⁴Note that the function $\text{rand}(0, 1)$ in steps 4 and 12 returns a random number uniformly distributed in the interval $[0, 1]$. Also, the function $\text{randi}(L_n^{\min}, L_n^{\max})$ in step 19 returns a random integer uniformly distributed in the set $\{L_n^{\min}, \dots, L_n^{\max}\}$. The outputs of different function calls are *independent*.

the integer/discrete constraints automatically, i.e., $\tilde{x}_n \in \{0, 1\}$ and $\tilde{L}_n \in \{L_n^{\min}, \dots, L_n^{\max}\}$ for every $n \in \mathcal{N}$.

Now, it remains to answer how close is the achieved objective value $\tilde{G} \triangleq G(\tilde{\mathbf{x}}, \tilde{\mathbf{L}})$ to the global minimum G^* , and whether or not the last three constraints, (17d), (17e) and (17f), are satisfied. Of course, there is no absolute/deterministic answer to these type of questions since $\tilde{\mathbf{x}}$ and $\tilde{\mathbf{L}}$ are random variables. Nevertheless, we can provide some (*a priori*) *probabilistic guarantees* on the algorithm's performance.

Theorem 2 (Expectation guarantees): The solution $(\tilde{\mathbf{x}}, \tilde{\mathbf{L}})$ of LPR-RA has the following properties:

$$\mathbb{E} \left(G(\tilde{\mathbf{x}}, \tilde{\mathbf{L}}) \right) = G^\dagger, \quad (27)$$

$$\mathbb{E} \left(\sum_{n \in \mathcal{N}} \tilde{x}_n \right) = \sum_{n \in \mathcal{N}} x_n^\dagger \leq M, \quad (28)$$

$$\mathbb{E} \left(L_{\text{tot}}(\tilde{\mathbf{x}}, \tilde{\mathbf{L}}) \right) = \sum_{n \in \mathcal{N}} z_n^\dagger \leq L_{\text{tot}}^{\max}, \quad (29)$$

$$\mathbb{E} \left(C_{\text{tot}}(\tilde{\mathbf{x}}, \tilde{\mathbf{L}}) \right) = \sum_{n \in \mathcal{N}} c_n x_n^\dagger + \sum_{n \in \mathcal{N}} \lambda_n z_n^\dagger \leq C_{\text{tot}}^{\max}. \quad (30)$$

Proof: See Appendix A. \square

In other words, the solution $(\tilde{\mathbf{x}}, \tilde{\mathbf{L}})$ satisfies *in expectation* the three constraints (17d)–(17f) and its objective value is *in expectation* equal to that of LPR.

Afterwards, we give some deviation guarantees using *concentration inequalities*, that is, probability bounds on how close a random variable is from some value (typically, its expectation).

Theorem 3 (Deviation guarantees): Let $\Delta_0 = \sum_{n \in \mathcal{N}} (\beta_n L_n^{\max})^2$, $\Delta_1 = N (\geq 1)$, $\Delta_2 = \sum_{n \in \mathcal{N}} (L_n^{\max})^2$ and $\Delta_3 = \sum_{n \in \mathcal{N}} (c_n + \lambda_n L_n^{\max})^2$ with $\Delta_0, \Delta_2, \Delta_3 > 0$. Then, the solution $(\tilde{\mathbf{x}}, \tilde{\mathbf{L}})$ achieved by Algorithm 2 satisfies the following probabilistic conditions:

$$\Pr(\mathcal{E}_k) \geq 1 - \xi, \quad \forall k \in \{0, 1, 2, 3\}, \quad (31)$$

where $\xi = (N + 1)^{-2} \in (0, 1/4]$ and the events $\{\mathcal{E}_k\}_{k=0}^3$ are defined by

$$\mathcal{E}_0 = \left\{ G(\tilde{\mathbf{x}}, \tilde{\mathbf{L}}) \leq G^* + \epsilon_0 \right\}, \quad (32)$$

$$\mathcal{E}_1 = \left\{ \sum_{n \in \mathcal{N}} \tilde{x}_n \leq M + \epsilon_1 \right\}, \quad (33)$$

$$\mathcal{E}_2 = \left\{ L_{\text{tot}}(\tilde{\mathbf{x}}, \tilde{\mathbf{L}}) \leq L_{\text{tot}}^{\max} + \epsilon_2 \right\}, \quad (34)$$

$$\mathcal{E}_3 = \left\{ C_{\text{tot}}(\tilde{\mathbf{x}}, \tilde{\mathbf{L}}) \leq C_{\text{tot}}^{\max} + \epsilon_3 \right\}, \quad (35)$$

with $\epsilon_k = \sqrt{\Delta_k \log(N + 1)} > 0$ for all $k \in \{0, 1, 2, 3\}$.

Furthermore, the approximate solution $(\tilde{\mathbf{x}}, \tilde{\mathbf{L}})$ satisfies the following inequalities (which are called *overall deviation guarantees*):

$$\Pr \left(\bigcap_{k=1}^3 \mathcal{E}_k \right) \geq 1 - \xi', \quad (36)$$

$$\Pr \left(\bigcap_{k=0}^3 \mathcal{E}_k \right) \geq 1 - \xi'', \quad (37)$$

where $\xi' = 3\xi = 3(N + 1)^{-2} \in (0, 3/4]$ and $\xi'' = 4\xi = 4(N + 1)^{-2} \in (0, 1]$.

Proof: See Appendix B. \square

In essence, ϵ_0 quantifies the deviation from the global optimum, while $\{\epsilon_k\}_{k=1}^3$ express the violation tolerance for each constraint. Moreover, (36) has to do with the satisfiability of the three constraints (17d)–(17f), while (37) includes additionally the objective value.

Notice that $\xi = \xi(N) = o(1)$, $\xi' = \xi'(N) = o(1)$ and $\xi'' = \xi''(N) = o(1)$.⁵ Therefore, an approximate solution satisfying any nonempty subset of $\{\mathcal{E}_k\}_{k=0}^3$ can be found *with high probability*, i.e., with probability $1 - o(1)$. However, observe that there is an inherent tradeoff between the probability bound $1 - \xi$ and a deviation tolerance ϵ_k , that is, both of them increase with N but with different growth rates.

Remark 5 (Performance improvement): In order to enhance the algorithm's performance (i.e., achieve better probability bounds), we can use multiple *i.i.d. rounding trials* at the cost of increased computational complexity. For example, let T be the number of rounding trials and $(\tilde{\mathbf{x}}^{(t)}, \tilde{\mathbf{L}}^{(t)})$ be the approximate solution obtained in rounding trial $t \in \{1, \dots, T\}$. Also, for every $k \in \{1, 2, 3\}$, let $\mathcal{E}_k^{(t)}$ be the event \mathcal{E}_k (see (33)–(35)) with $(\tilde{\mathbf{x}}, \tilde{\mathbf{L}})$ replaced by $(\tilde{\mathbf{x}}^{(t)}, \tilde{\mathbf{L}}^{(t)})$. Then, the probability of finding at least one approximate solution $(\tilde{\mathbf{x}}^{(t)}, \tilde{\mathbf{L}}^{(t)})$ satisfying all the events $\{\mathcal{E}_k^{(t)}\}_{k=1}^3$, within T rounding trials, is lower bounded by

$$\begin{aligned} \Pr \left(\bigcup_{t=1}^T \left(\bigcap_{k=1}^3 \mathcal{E}_k^{(t)} \right) \right) &= 1 - \Pr \left(\bigcap_{t=1}^T \left(\bigcup_{k=1}^3 (\mathcal{E}_k^{(t)})^c \right) \right) \\ &= 1 - \prod_{t=1}^T \Pr \left(\bigcup_{k=1}^3 (\mathcal{E}_k^{(t)})^c \right) \\ &= 1 - \left[\Pr \left(\bigcup_{k=1}^3 \mathcal{E}_k^c \right) \right]^T \\ &= 1 - \left[1 - \Pr \left(\bigcap_{k=1}^3 \mathcal{E}_k \right) \right]^T \\ &\geq 1 - \xi'^T, \end{aligned} \quad (38)$$

where the first and fourth equalities are because of De Morgan's law, the second and third equalities follows from the i.i.d. assumption of rounding trials, while the last inequality is due to (36). It is not hard to see that, given $\xi' \in (0, 3/4]$, this probability tends to 1 as $T \rightarrow \infty$.

Concerning the complexity of Algorithm 2, the LPR problem requires $O(N^{3.5})$ time, while the computation of $(\tilde{\mathbf{x}}, \tilde{\mathbf{L}})$ takes $\Theta(N)$ time. As a result, the total complexity of LPR-RA is $O(N^{3.5} + N) = O(N^{3.5})$, that is, asymptotically the same (up to a constant) as that of LPR and LPR-GA. In

⁵Here, the asymptotic term $o(1)$ is defined for $N \rightarrow \infty$, for example, $\xi = \xi(N) = o(1)$ means that $\lim_{N \rightarrow \infty} \xi = 0$.

TABLE I
COMPLEXITY & PERFORMANCE OF OPTIMIZATION ALGORITHMS

Optimization algorithm	Computational complexity	Performance guarantee
Exhaustive enumeration	$\Theta \left(\sum_{\substack{\mathcal{I} \subseteq \mathcal{N} \\ \mathcal{I} \leq M}} \mathcal{I} \prod_{i \in \mathcal{I}} R_i \right)$, where, for all $n \in \mathcal{N}$, $R_n = L_n^{\max} - L_n^{\min} + 1$	Globally optimal solution
LPR	$O(N^{3.5})$	Lower bound
LPR-GA (Algorithm 1)	$O(N^{3.5})$	Feasible solution
LPR-RA (Algorithm 2)	$O(N^{3.5})$ or $O(N^{3.5} + NT)$, where T is the number of i.i.d. rounding trials	Approximate solution with probabilistic performance guarantees (see Theorems 2 and 3 as well as Remark 5)
AEGA* (Benchmark I)	$O(N \log N)$	Feasible solution
MEGA* (Benchmark II)	$O(N \log N)$	Feasible solution

* These heuristic algorithms are described in Section V-B.

case of T i.i.d. rounding trials (see Remark 5), the computational complexity increases to $O(N^{3.5} + NT)$. Finally, the complexity and performance of all optimization algorithms are summarized in Table I.

V. NUMERICAL RESULTS AND DISCUSSION

The main objective of this section is twofold: the first is to compare the performance of optimization algorithms (in terms of the upper bound of system outage probability) and the second is the comparison between FD and HD schemes.

A. Simulation Setup

We generate random system configurations, where UE-1 and UE-2 are constantly located at $(0, 0)$ and $(100, 0)$, respectively, while each IRS location is uniformly distributed either inside the rectangle $[30, 70] \times [20, 40]$ or $[30, 70] \times [-40, -20]$, with probability 1/2 of being in each rectangle.⁶ Unless otherwise stated, the system parameters are presented in Table II; the positions of UEs and IRSs are on the x-y plane and all coordinates are expressed in meters. Note that, for a given problem, the IRS locations and $\{c_n, \lambda_n\}_{n \in \mathcal{N}}$ are all fixed (the randomization is only used for problem generation). In addition, all figures present average values obtained from 10^3 independent simulation scenarios. Also, the LPR problem (22) is solved using CVX software [31] with SDPT3 solver [32].

Moreover, for every problem instance, LPR-RA performs a maximum number of i.i.d. rounding trials, T_{\max} , in order to increase the probability of achieving a feasible solution. In particular, Algorithm 2 generates independent approximate solutions successively and terminates either when a feasible solution is found or when the maximum number of trials is reached. In all figure captions, we have included the percentage

⁶Here, the IRSs are distributed in the 2D-space for the sake of simplicity. Nevertheless, the proposed methodology is straightforwardly applicable to 3D-space scenarios, where the IRSs may be located at different heights.

TABLE II
SIMULATION PARAMETERS

Parameter	Value
Positions of UEs	$(0, 0), (100, 0)$
Transmit power of UEs, P	25 dBm
Channel variance, σ^2	1
Residual-LI power, σ_{LI}^2	-70 dBm
Noise power, σ_w^2	-80 dBm
SINR threshold, γ_{th}	8 dB
Path-loss model parameters (where the distance is measured in meters)	$A_0 = 1, \alpha = 2.7$
IRS location	Uniform $([30, 70] \times [20, 40])$ or Uniform $([30, 70] \times [-40, -20])$ with probability 1/2
Number of available IRS locations, N	25
Maximum number of installed IRSs, M	7
Minimum number of reflecting elements for each IRS, $L_n^{\min} = L^{\min}, \forall n \in \mathcal{N}$	5
Maximum number of reflecting elements for each IRS, $L_n^{\max} = L^{\max}, \forall n \in \mathcal{N}$	40
Maximum total number of reflecting elements, L_{tot}^{\max}	250
Maximum total IRS installation cost, C_{tot}^{\max}	75
IRS fixed deployment cost, c_n	Uniform $([1, 5])$
IRS cost rate, λ_n	Uniform $([0.1, 0.5])$
Maximum number of i.i.d. rounding trials for LPR-RA, T_{\max}	50

of problems for which LPR-RA returned a feasible solution, within the maximum number of rounding trials.

Despite the fact that a comparison with the optimum value would have been useful, this does not appear in the numerical results because the complexity of the exhaustive-enumeration algorithm is extremely high. For example, consider a problem with $N = 25$, $M = 7$, $L^{\min} = 5$ and $L^{\max} = 40$ (as shown in Table II). In this case, the exhaustive-enumeration algorithm would require at least $\binom{N}{M} M R^M \approx 2.637 \times 10^{17}$ arithmetic operations, where $R = L^{\max} - L^{\min} + 1$ (cf. Section IV-A). If each operation takes approximately 1 μs , then the algorithm's runtime (for a *single* problem) is roughly 7.325×10^7 hr $\approx 3.052 \times 10^6$ d $\approx 8.362 \times 10^3$ yr, which is obviously prohibitive.

Nevertheless, we definitely know that the minimum value always lies between LPR (lower bound) and LPR-GA (upper bound, since its solution is guaranteed to be feasible), that is, $G^\dagger \leq G^* \leq G'$. Similar inequalities also hold for the upper bound of system outage probability, $\bar{P}_{\text{out}}(\cdot)$, due to the monotonicity of exponential function; recall that $G(\cdot) = \log(\bar{P}_{\text{out}}(\cdot))$.

B. Baseline Schemes (Benchmarks)

In order to evaluate the performance of the proposed algorithms, we consider (besides the lower bound obtained from LPR) two baseline schemes:

- *Average-element greedy algorithm (AEGA)*: First, the number of reflecting elements L_n is set equal to $L_n^{\text{avg}} \triangleq$

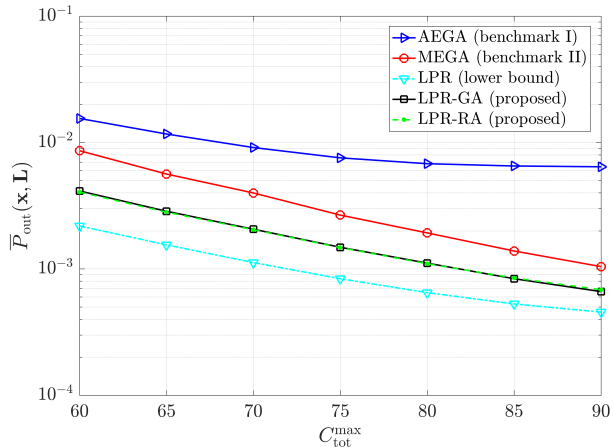


Fig. 2. Upper bound of system outage probability versus the maximum total IRS installation cost. The percentage of problems for which LPR-RA has achieved a feasible solution is [98.5, 98.4, 99.3, 98.6, 99.1, 99.2, 99.5]% for each value of $C_{\text{tot}}^{\text{max}}$, respectively.

$\lceil \frac{1}{2}(L_n^{\min} + L_n^{\max}) \rceil \in \{L_n^{\min}, \dots, L_n^{\max}\}$ for all $n \in \mathcal{N}$. Then, we sort the IRS locations in ascending order in terms of the product $\beta_n L_n^{\text{avg}}$ (≤ 0). Let $(\sigma_1, \dots, \sigma_N) \in \Sigma_{\mathcal{N}}$ be the order of IRS locations after sorting, where $\Sigma_{\mathcal{N}}$ is the set of all permutations of \mathcal{N} , therefore $\beta_{\sigma_1} L_{\sigma_1}^{\text{avg}} \leq \dots \leq \beta_{\sigma_N} L_{\sigma_N}^{\text{avg}}$. Finally, AEGA follows the steps 12–20 of Algorithm 1 (LPR-GA) to compute the binary vector \mathbf{x} . In essence, this algorithm can be seen as a greedy procedure that consecutively selects the IRS location inducing the maximum decrease in the objective value (i.e., the upper bound of system outage probability), among the IRS locations not selected yet, while satisfying all constraints.

- *Maximum-element greedy algorithm (MEGA)*: This algorithm follows the same procedure as AEGA by replacing L_n^{avg} with L_n^{max} , for all $n \in \mathcal{N}$.

Both methods are heuristic algorithms (i.e., without a priori performance guarantees) with computational complexity $O(N \log N)$ because of the sorting procedure. In addition, they always find a feasible solution due to their design.

C. Performance Comparison of Optimization Algorithms

Subsequently, the performance of optimization algorithms is examined by varying the maximum total IRS installation cost, the maximum number of reflecting elements, the number of available IRS locations as well as the SINR threshold.

1) Impact of the Maximum Total IRS Installation Cost:

Fig. 2 shows the upper bound of system outage probability, against the maximum total IRS installation cost, achieved by AEGA, MEGA, LPR, LPR-GA (Algorithm 1) and LPR-RA (Algorithm 2). As expected, the outage probability is a nonincreasing function of $C_{\text{tot}}^{\text{max}}$ for all algorithms, since larger $C_{\text{tot}}^{\text{max}}$ translates to a less restricted feasible set. Furthermore, the proposed algorithms, LPR-GA and LPR-RA, achieve higher performance than the two benchmarks, AEGA and MEGA (with AEGA having the worst performance). It is interesting to observe that LPR-GA and LPR-RA exhibit very

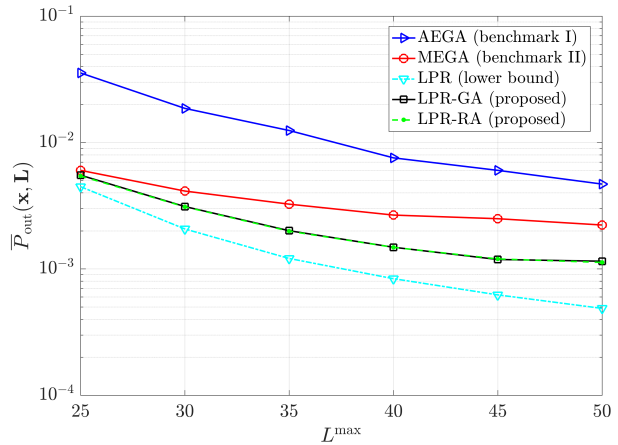


Fig. 3. Upper bound of system outage probability versus the maximum number of reflecting elements. The percentage of problems for which LPR-RA has found a feasible solution is [98.7, 98.4, 98.1, 98.3, 99.6, 98.3]% for each value of L^{max} , respectively.

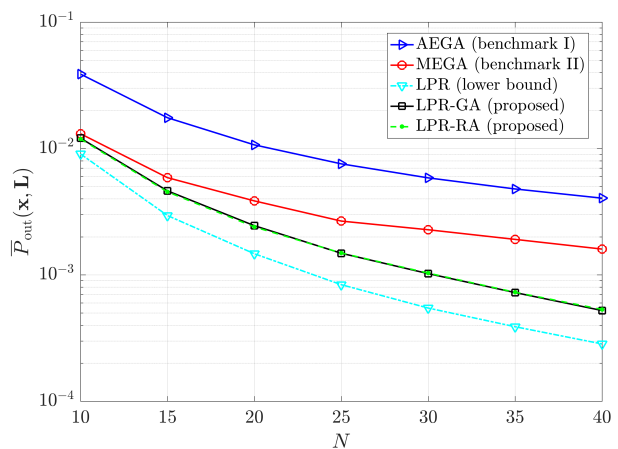


Fig. 4. Upper bound of system outage probability versus the number of available IRS locations. The percentage of problems for which LPR-RA has returned a feasible solution is [97.7, 98.2, 98.5, 98.9, 99.1, 98.7, 99.6]% for each value of N , respectively.

similar (almost identical) performance, which is very close to the lower bound of LPR. Intuitively, we anticipate such behavior because both algorithms rely on LPR. Finally, LPR-RA demonstrates extremely high percentage (above 98%) of achieving a feasible solution within $T_{\text{max}} = 50$ rounding trials.

2) *Impact of the Maximum Number of Reflecting Elements*: The effect of the maximum number of reflecting elements (for each IRS) on the system outage probability is presented in Fig. 3. Similar conclusions with Fig. 2 can be drawn here as well. In addition, MEGA performs slightly worse than LPR-GA and LPR-RA for small values of L^{max} (e.g., 25 and 30), whereas their difference in performance becomes more apparent as L^{max} increases.

3) Impact of the Number of Available IRS Locations:

Fig. 4 illustrates the system outage probability as a function of the number of candidate locations for installing an IRS. More specifically, we can observe that, as N increases, all algorithms achieve lower outage probability because there are

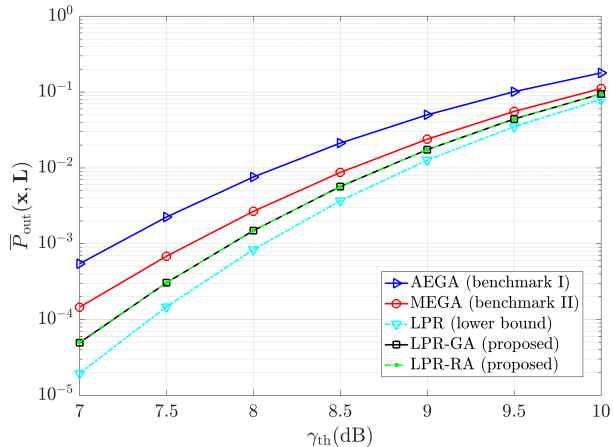


Fig. 5. Upper bound of system outage probability versus the SINR threshold. The percentage of problems for which LPR-RA has achieved a feasible solution is [99.1, 98.9, 98.6, 98.5, 99.2, 98.4, 98.4]% for each value of γ_{th} , respectively.

more options available for the IRS deployment. Once again, the proposed algorithms (LPR-GA and LPR-RA) significantly outperform the baseline schemes, especially when N is relatively large, and remain very close to the lower bound (and, thus, to the global minimum) for all values of N . The latter demonstrates the robustness of the developed algorithms in terms of the size of the search space (cf. Figs. 2 and 3).

4) Impact of the SINR Threshold:

The upper bound of system outage probability versus the SINR threshold is shown in Fig. 5. In particular, the outage probability increases with γ_{th} for all optimization algorithms, which is intuitively expected. Furthermore, it is interesting to note that the distance of the objective value achieved by AEGA, MEGA, LPR-GA, LPR-RA from the lower bound decreases as the SINR threshold increases. Roughly speaking, this means that the achieved solution tends to be globally optimal, especially for LPR-GA and LPR-RA.

D. Comparison between FD and HD Systems

Afterwards, the optimization algorithms are used in order to make meaningful comparisons between FD and HD wireless technologies.⁷

1) Impact of the Transmit Power of UEs:

Firstly, let us examine the effect of the transmit power of UEs on the system outage probability. According to Fig. 6, the proposed optimization algorithms perform much better than the two benchmarks, especially for high transmit power, in both HD and FD schemes. In addition, we can observe that FD is superior to HD system (in terms of outage probability) when $P < 26$ dBm, irrespective of the algorithm used for comparison. On the other hand, FD is inferior to HD scheme when $P > 26$ dBm.

2) Impact of the Residual-LI Power:

Secondly, we study how the residual-LI power affects the system outage probability, assuming constant transmit power.

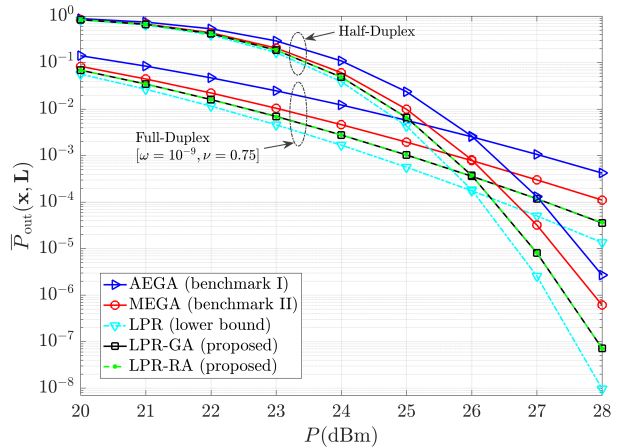


Fig. 6. Upper bound of system outage probability versus the transmit power of UEs for $\gamma_{th} = 9$ dB; $\sigma_{LI}^2 = \omega P^\nu$ in FD scheme, whereas $\sigma_{LI}^2 = 0$ in HD scheme. The percentage of problems for which LPR-RA has found a feasible solution is [98.3, 98.6, 98.6, 98.0, 99.1, 99.1, 98.6, 98.8, 99.2]% in FD system and [97.7, 98.3, 98.3, 99.1, 99.1, 98.3, 98.7, 99.0, 99.4]% in HD system for each value of P , respectively.

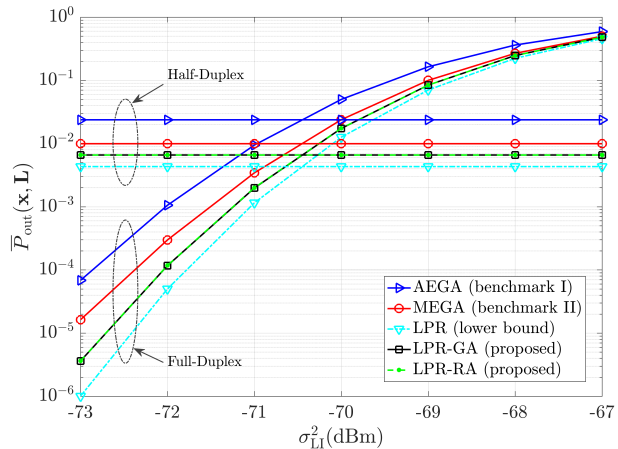


Fig. 7. Upper bound of system outage probability versus the residual-LI power at each UE for $\gamma_{th} = 9$ dB; the transmit power is fixed at $P = 25$ dBm. The percentage of problems for which LPR-RA has returned a feasible solution is [99.0, 98.9, 98.7, 98.9, 98.7, 98.5, 98.9]% in FD system for each value of σ_{LI}^2 , respectively, and 98.6% in HD system regardless of σ_{LI}^2 .

Based on Fig. 7, it is obvious that LPR-GA and LPR-RA again show better performance compared to the baseline schemes, not only in FD but also in HD scenario. Moreover, for the FD scheme, the upper bound of system outage probability increases rapidly with the residual-LI power. Finally, FD outperforms HD system when σ_{LI}^2 is approximately less than -70.4 dBm, whereas HD is preferable when σ_{LI}^2 is greater than -70.4 dBm (regardless of the comparison algorithm). In other words, FD is more beneficial than HD technology, provided that the LI at each UE is sufficiently suppressed.

VI. CONCLUSION

In this paper, we have dealt with the minimization of outage probability in a two-way FD communication system assisted by multiple IRSs. In particular, we have transformed the joint

⁷For details on the HD scheme, see Section II-D.

IRS location and size optimization problem into a discrete problem, which turned out to be NP-hard. In order to overcome this difficulty, two efficient (polynomial-time) algorithms have been proposed, which are based on the solution of LPR. The first is a deterministic greedy method, while the second is a randomized approximation algorithm. According to the numerical results, the developed algorithms have shown much higher performance than the benchmarks. Their achieved objective values have also been very close to the lower bound and, therefore, to the global minimum. Moreover, we have observed that FD outperforms HD scheme, provided that the LI at both UEs is adequately mitigated; this is in line with our intuition.

APPENDIX A PROOF OF THEOREM 2

First of all, due to (24)–(26), we have that

$$\mathbb{E}(\tilde{x}_n) = 1 \cdot x_n^\dagger + 0 \cdot (1 - x_n^\dagger) = x_n^\dagger, \quad (39)$$

$$\begin{aligned} \mathbb{E}(\tilde{L}_n | x_n^\dagger \neq 0) &= (\lfloor L_n^\dagger \rfloor + 1) \text{frac}(L_n^\dagger) \\ &\quad + \lfloor L_n^\dagger \rfloor (1 - \text{frac}(L_n^\dagger)) \\ &= \text{frac}(L_n^\dagger) + \lfloor L_n^\dagger \rfloor = L_n^\dagger, \end{aligned} \quad (40)$$

$$\begin{aligned} \mathbb{E}(\tilde{L}_n | x_n^\dagger = 0) &= \frac{1}{L_n^{\max} - L_n^{\min} + 1} \sum_{i=L_n^{\min}}^{L_n^{\max}} i \\ &= \frac{1}{2}(L_n^{\min} + L_n^{\max}). \end{aligned} \quad (41)$$

Furthermore, by defining the random variable $\tilde{z}_n = \tilde{x}_n \tilde{L}_n$ for all $n \in \mathcal{N}$ and exploiting the independency of \tilde{x}_n and \tilde{L}_n , we get the following conditional expectations:

$$\begin{aligned} \mathbb{E}(\tilde{z}_n | x_n^\dagger \neq 0) &= \mathbb{E}(\tilde{x}_n | x_n^\dagger \neq 0) \mathbb{E}(\tilde{L}_n | x_n^\dagger \neq 0) \\ &= x_n^\dagger L_n^\dagger = z_n^\dagger, \end{aligned} \quad (42)$$

$$\begin{aligned} \mathbb{E}(\tilde{z}_n | x_n^\dagger = 0) &= \mathbb{E}(\tilde{x}_n | x_n^\dagger = 0) \mathbb{E}(\tilde{L}_n | x_n^\dagger = 0) \\ &= 0 \cdot \frac{1}{2}(L_n^{\min} + L_n^{\max}) = 0 = z_n^\dagger, \end{aligned} \quad (43)$$

where the latter is based on the fact that: if $x_n^\dagger = 0$, then $z_n^\dagger = 0$ and $\tilde{x}_n = 0$. As a result, combining the above equations, $\mathbb{E}(\tilde{z}_n) = z_n^\dagger$ for all $n \in \mathcal{N}$.

Because of the linearity of expectation and the feasibility of $(\mathbf{x}^\dagger, \mathbf{z}^\dagger)$, we obtain

$$\begin{aligned} \mathbb{E}(G(\tilde{\mathbf{x}}, \tilde{\mathbf{L}})) &= \mathbb{E}\left(\sum_{n \in \mathcal{N}} \beta_n \tilde{z}_n\right) = \sum_{n \in \mathcal{N}} \beta_n \mathbb{E}(\tilde{z}_n) \\ &= \sum_{n \in \mathcal{N}} \beta_n z_n^\dagger = G^\dagger, \end{aligned} \quad (44)$$

$$\mathbb{E}\left(\sum_{n \in \mathcal{N}} \tilde{x}_n\right) = \sum_{n \in \mathcal{N}} \mathbb{E}(\tilde{x}_n) = \sum_{n \in \mathcal{N}} x_n^\dagger \leq M, \quad (45)$$

$$\begin{aligned} \mathbb{E}(L_{\text{tot}}(\tilde{\mathbf{x}}, \tilde{\mathbf{L}})) &= \mathbb{E}\left(\sum_{n \in \mathcal{N}} \tilde{z}_n\right) = \sum_{n \in \mathcal{N}} \mathbb{E}(\tilde{z}_n) \\ &= \sum_{n \in \mathcal{N}} z_n^\dagger \leq L_{\text{tot}}^{\max}, \end{aligned} \quad (46)$$

$$\begin{aligned} \mathbb{E}(C_{\text{tot}}(\tilde{\mathbf{x}}, \tilde{\mathbf{L}})) &= \mathbb{E}\left(\sum_{n \in \mathcal{N}} c_n \tilde{x}_n + \sum_{n \in \mathcal{N}} \lambda_n \tilde{z}_n\right) \\ &= \sum_{n \in \mathcal{N}} c_n \mathbb{E}(\tilde{x}_n) + \sum_{n \in \mathcal{N}} \lambda_n \mathbb{E}(\tilde{z}_n) \\ &= \sum_{n \in \mathcal{N}} c_n x_n^\dagger + \sum_{n \in \mathcal{N}} \lambda_n z_n^\dagger \leq C_{\text{tot}}^{\max}. \end{aligned} \quad (47)$$

Therefore, Theorem 2 has been proven.

APPENDIX B PROOF OF THEOREM 3

In order to prove Theorem 3, we make use of a concentration inequality for sums of independent and bounded random variables, namely, Hoeffding's inequality. This is a generalization of the well-known Chernoff bound, which applies to Bernoulli random variables.

Lemma 1 (Hoeffding's inequality [33]): Let $\{X_n\}_{n \in \mathcal{N}}$ be a finite set of independent random variables, with $X_n \in [a_n, b_n]$ for all $n \in \mathcal{N}$ (where $a_n \leq b_n$), and $X \triangleq \sum_{n \in \mathcal{N}} X_n$. Then, for any $u > 0$,

$$\Pr(X - \mathbb{E}(X) > u) \leq e^{-2u^2/\Delta}, \quad (48)$$

where $\Delta = \sum_{n \in \mathcal{N}} (b_n - a_n)^2$.

The probability of approximating the optimum value within a given tolerance $\epsilon_0 > 0$ is lower bounded by

$$\begin{aligned} \Pr(G(\tilde{\mathbf{x}}, \tilde{\mathbf{L}}) \leq G^* + \epsilon_0) &= 1 - \Pr(G(\tilde{\mathbf{x}}, \tilde{\mathbf{L}}) > G^* + \epsilon_0) \\ &\geq 1 - \Pr(G(\tilde{\mathbf{x}}, \tilde{\mathbf{L}}) > G^\dagger + \epsilon_0) \\ &\geq 1 - e^{-2\epsilon_0^2/\Delta_0}, \end{aligned} \quad (49)$$

where $\Delta_0 = \sum_{n \in \mathcal{N}} (\beta_n L_n^{\max})^2$. Here, the first inequality is because $G^\dagger \leq G^*$, while the second inequality follows from Lemma 1 by taking advantage of (27) and noticing that $G(\tilde{\mathbf{x}}, \tilde{\mathbf{L}}) = \sum_{n \in \mathcal{N}} \beta_n (\tilde{x}_n \tilde{L}_n) = \sum_{n \in \mathcal{N}} \beta_n \tilde{z}_n$ is the sum of independent random variables $\{\beta_n \tilde{z}_n\}_{n \in \mathcal{N}}$ with $\beta_n \tilde{z}_n \in [\beta_n L_n^{\max}, 0]$; recall that $\beta_n \leq 0$. By assuming $\Delta_0 > 0$ and setting $\epsilon_0 = \sqrt{\Delta_0 \log(N+1)} > 0$, we get (31) for $k = 0$.

Regarding the probabilistic guarantee for the IRS-cardinality constraint, we have for any $\epsilon_1 > 0$

$$\begin{aligned} \Pr\left(\sum_{n \in \mathcal{N}} \tilde{x}_n \leq M + \epsilon_1\right) &= 1 - \Pr\left(\sum_{n \in \mathcal{N}} \tilde{x}_n > M + \epsilon_1\right) \\ &\geq 1 - \Pr\left(\sum_{n \in \mathcal{N}} \tilde{x}_n > \sum_{n \in \mathcal{N}} x_n^\dagger + \epsilon_1\right) \\ &\geq 1 - e^{-2\epsilon_1^2/\Delta_1}, \end{aligned} \quad (50)$$

where $\Delta_1 = N$. The two inequalities follows from (28) and Lemma 1. Finally, by choosing $\epsilon_1 = \sqrt{\Delta_1 \log(N+1)} > 0$ we obtain (31) for $k = 1$.

Moreover, based on (29) and Lemma 1, we obtain for any $\epsilon_2 > 0$

$$\begin{aligned} \Pr\left(L_{\text{tot}}(\tilde{\mathbf{x}}, \tilde{\mathbf{L}}) \leq L_{\text{tot}}^{\max} + \epsilon_2\right) &= 1 - \Pr\left(L_{\text{tot}}(\tilde{\mathbf{x}}, \tilde{\mathbf{L}}) > L_{\text{tot}}^{\max} + \epsilon_2\right) \\ &\geq 1 - \Pr\left(L_{\text{tot}}(\tilde{\mathbf{x}}, \tilde{\mathbf{L}}) > \sum_{n \in \mathcal{N}} z_n^\dagger + \epsilon_2\right) \\ &\geq 1 - e^{-2\epsilon_2^2/\Delta_2}, \end{aligned} \quad (51)$$

where $\Delta_2 = \sum_{n \in \mathcal{N}} (L_n^{\max})^2$. Note that $L_{\text{tot}}(\tilde{\mathbf{x}}, \tilde{\mathbf{L}}) = \sum_{n \in \mathcal{N}} \tilde{x}_n \tilde{L}_n = \sum_{n \in \mathcal{N}} \tilde{z}_n$ is the sum of independent random variables $\{\tilde{z}_n\}_{n \in \mathcal{N}}$ with $\tilde{z}_n \in [0, L_n^{\max}]$. Inequality (31) for $k = 2$ can be easily derived, assuming $\Delta_2 > 0$ and setting $\epsilon_2 = \sqrt{\Delta_2 \log(N+1)} > 0$.

Although \tilde{x}_n and $\tilde{z}_n = \tilde{x}_n \tilde{L}_n$ are not independent random variables, $C_{\text{tot}}(\tilde{\mathbf{x}}, \tilde{\mathbf{L}}) = \sum_{n \in \mathcal{N}} c_n \tilde{x}_n + \sum_{n \in \mathcal{N}} \lambda_n (\tilde{x}_n \tilde{L}_n)$ can be written as the sum of independent random variables $\{(c_n + \lambda_n \tilde{L}_n) \tilde{x}_n\}_{n \in \mathcal{N}}$, i.e., $C_{\text{tot}}(\tilde{\mathbf{x}}, \tilde{\mathbf{L}}) = \sum_{n \in \mathcal{N}} (c_n + \lambda_n \tilde{L}_n) \tilde{x}_n$, with $(c_n + \lambda_n \tilde{L}_n) \tilde{x}_n \in [0, c_n + \lambda_n L_n^{\max}]$. As a consequence, for any $\epsilon_3 > 0$, the probability of the event \mathcal{E}_3 can be lower bounded by

$$\begin{aligned} \Pr\left(C_{\text{tot}}(\tilde{\mathbf{x}}, \tilde{\mathbf{L}}) \leq C_{\text{tot}}^{\max} + \epsilon_3\right) &= 1 - \Pr\left(C_{\text{tot}}(\tilde{\mathbf{x}}, \tilde{\mathbf{L}}) > C_{\text{tot}}^{\max} + \epsilon_3\right) \\ &\geq 1 - \Pr\left(C_{\text{tot}}(\tilde{\mathbf{x}}, \tilde{\mathbf{L}}) > \sum_{n \in \mathcal{N}} c_n x_n^\dagger \right. \\ &\quad \left. + \sum_{n \in \mathcal{N}} \lambda_n z_n^\dagger + \epsilon_3\right) \\ &\geq 1 - e^{-2\epsilon_3^2/\Delta_3}, \end{aligned} \quad (52)$$

where $\Delta_3 = \sum_{n \in \mathcal{N}} (c_n + \lambda_n L_n^{\max})^2$, while the two inequalities result from the combination of (30) with Lemma 1. Assuming $\Delta_3 > 0$ and choosing $\epsilon_3 = \sqrt{\Delta_3 \log(N+1)} > 0$, we have (31) for $k = 3$. Hence, (31) has been proven for all $k \in \{0, 1, 2, 3\}$.

Now, let us consider inequality (36). By applying *De Morgan's law* and the *union bound theorem*, we obtain

$$\Pr\left(\bigcap_{k=1}^3 \mathcal{E}_k\right) = 1 - \Pr\left(\left(\bigcap_{k=1}^3 \mathcal{E}_k\right)^c\right) = 1 - \Pr\left(\bigcup_{k=1}^3 \mathcal{E}_k^c\right), \quad (53)$$

$$\Pr\left(\bigcup_{k=1}^3 \mathcal{E}_k^c\right) \leq \sum_{k=1}^3 \Pr(\mathcal{E}_k^c) = \sum_{k=1}^3 (1 - \Pr(\mathcal{E}_k)). \quad (54)$$

Subsequently, by combining the above equations and leveraging (31), we deduce

$$\begin{aligned} \Pr\left(\bigcap_{k=1}^3 \mathcal{E}_k\right) &\geq 1 - \sum_{k=1}^3 (1 - \Pr(\mathcal{E}_k)) \\ &\geq 1 - 3\xi = 1 - \xi'. \end{aligned} \quad (55)$$

Finally, inequality (37) can be derived by following similar steps as above, so Theorem 3 follows immediately.

REFERENCES

- [1] C. N. Efrem and I. Krikidis, "IRS deployment optimization in multi-IRS assisted two-way full-duplex communication systems," *IEEE International Conference on Communications (ICC)*, Seoul, South Korea, May 2022, pp. 1-6.
- [2] M. Di Renzo *et al.*, "Smart radio environments empowered by reconfigurable AI meta-surfaces: An idea whose time has come," *EURASIP Journal on Wireless Communications and Networking*, vol. 129, no. 1, May 2019.
- [3] Q. Wu and R. Zhang, "Towards smart and reconfigurable environment: Intelligent reflecting surface aided wireless network," *IEEE Communications Magazine*, vol. 58, no. 1, pp. 106-112, January 2020.
- [4] C. Huang *et al.*, "Holographic MIMO surfaces for 6G wireless networks: Opportunities, challenges, and trends," *IEEE Wireless Communications*, vol. 27, no. 5, pp. 118-125, October 2020.
- [5] M. Di Renzo *et al.*, "Smart radio environments empowered by reconfigurable intelligent surfaces: How it works, state of research, and the road ahead," *IEEE Journal on Selected Areas in Communications*, vol. 38, no. 11, pp. 2450-2525, Nov. 2020.
- [6] Q. Wu, S. Zhang, B. Zheng, C. You and R. Zhang, "Intelligent reflecting surface-aided wireless communications: A tutorial," *IEEE Transactions on Communications*, vol. 69, no. 5, pp. 3313-3351, May 2021.
- [7] A. Sabharwal, P. Schniter, D. Guo, D. W. Bliss, S. Rangarajan and R. Wichman, "In-band full-duplex wireless: Challenges and opportunities," *IEEE Journal on Selected Areas in Communications*, vol. 32, no. 9, pp. 1637-1652, Sept. 2014.
- [8] Z. Zhang, X. Chai, K. Long, A. V. Vasilakos and L. Hanzo, "Full duplex techniques for 5G networks: Self-interference cancellation, protocol design, and relay selection," *IEEE Communications Magazine*, vol. 53, no. 5, pp. 128-137, May 2015.
- [9] G. Liu, F. R. Yu, H. Ji, V. C. M. Leung and X. Li, "In-band full-duplex relaying: A survey, research issues and challenges," *IEEE Communications Surveys & Tutorials*, vol. 17, no. 2, pp. 500-524, 2015.
- [10] G. Pan, J. Ye, J. An, and M.-S. Alouini, "Full-duplex enabled intelligent reflecting surface systems: Opportunities and challenges," *IEEE Wireless Communications*, vol. 28, no. 3, pp. 122-129, June 2021.
- [11] S. Atapattu, R. Fan, P. Dharmawansa, G. Wang, J. Evans and T. A. Tsiftsis, "Reconfigurable intelligent surface assisted two-way communications: Performance analysis and optimization," *IEEE Transactions on Communications*, vol. 68, no. 10, pp. 6552-6567, Oct. 2020.
- [12] Z. Abdullah, G. Chen, S. Lambotaran and J. A. Chambers, "Optimization of intelligent reflecting surface assisted full-duplex relay networks," *IEEE Wireless Commun. Lett.*, vol. 10, no. 2, pp. 363-367, Feb. 2021.
- [13] Z. Peng, Z. Zhang, C. Pan, L. Li and A. L. Swindlehurst, "Multiuser full-duplex two-way communications via intelligent reflecting surface," *IEEE Transactions on Signal Processing*, vol. 69, pp. 837-851, 2021.
- [14] M. A. Saeidi, M. J. Emadi, H. Masoumi, M. R. Mili, D. W. K. Ng and I. Krikidis, "Weighted sum-rate maximization for multi-IRS-assisted full-duplex systems with hardware impairments," *IEEE Transactions on Cognitive Communications and Networking*, vol. 7, no. 2, pp. 466-481, June 2021.
- [15] Y. Zhang, C. Zhong, Z. Zhang and W. Lu, "Sum rate optimization for two way communications with intelligent reflecting surface," *IEEE Communications Letters*, vol. 24, no. 5, pp. 1090-1094, May 2020.
- [16] D. Xu, X. Yu, Y. Sun, D. W. K. Ng and R. Schober, "Resource allocation for IRS-assisted full-duplex cognitive radio systems," *IEEE Transactions on Communications*, vol. 68, no. 12, pp. 7376-7394, Dec. 2020.
- [17] H. Lu, Y. Zeng, S. Jin and R. Zhang, "Aerial intelligent reflecting surface: Joint placement and passive beamforming design with 3D beam flattening," *IEEE Transactions on Wireless Communications*, vol. 20, no. 7, pp. 4128-4143, July 2021.
- [18] X. Mu, Y. Liu, L. Guo, J. Lin and R. Schober, "Joint deployment and multiple access design for intelligent reflecting surface assisted networks," *IEEE Transactions on Wireless Communications*, doi: 10.1109/TWC.2021.3075885.
- [19] X. Liu, Y. Liu, Y. Chen and H. V. Poor, "RIS enhanced massive non-orthogonal multiple access networks: Deployment and passive beamforming design," *IEEE Journal on Selected Areas in Communications*, vol. 39, no. 4, pp. 1057-1071, April 2021.
- [20] S. Zeng, H. Zhang, B. Di, Z. Han and L. Song, "Reconfigurable intelligent surface (RIS) assisted wireless coverage extension: RIS orientation and location optimization," *IEEE Communications Letters*, vol. 25, no. 1, pp. 269-273, Jan. 2021.
- [21] A. Zappone, M. Di Renzo, X. Xi and M. Debbah, "On the optimal number of reflecting elements for reconfigurable intelligent surfaces," *IEEE Wireless Commun. Lett.*, vol. 10, no. 3, pp. 464-468, March 2021.
- [22] B. Yu, L. Yang, X. Cheng and R. Cao, "Power and location optimization for full-duplex decode-and-forward relaying," *IEEE Transactions on Communications*, vol. 63, no. 12, pp. 4743-4753, Dec. 2015.
- [23] S. Li *et al.*, "Full-duplex amplify-and-forward relaying: Power and location optimization," *IEEE Transactions on Vehicular Technology*, vol. 66, no. 9, pp. 8458-8468, Sept. 2017.

- [24] J. Hou, S. Narayanan, N. Yi, Y. Ma and M. Shikh-Bahaei, "Symbol-level selective full-duplex relaying with power and location optimization," *IEEE Trans. Commun.*, vol. 66, no. 11, pp. 5097-5111, Nov. 2018.
- [25] N. K. Lyras, C. N. Efrem, C. I. Kourogiorgas and A. D. Panagopoulos, "Optimum monthly-based selection of ground stations for optical satellite networks," *IEEE Communications Letters*, vol. 22, no. 6, pp. 1192-1195, June 2018.
- [26] N. K. Lyras, C. N. Efrem, C. I. Kourogiorgas, A. D. Panagopoulos and P.-D. Arapoglou, "Optimizing the ground network of optical MEO satellite communication systems," *IEEE Systems Journal*, vol. 14, no. 3, pp. 3968-3976, Sept. 2020.
- [27] C. N. Efrem and A. D. Panagopoulos, "Globally optimal selection of ground stations in satellite systems with site diversity," *IEEE Wireless Communications Letters*, vol. 9, no. 7, pp. 1101-1104, July 2020.
- [28] C. N. Efrem and A. D. Panagopoulos, "Minimizing the installation cost of ground stations in satellite networks: Complexity, dynamic programming and approximation algorithm," *IEEE Wireless Communications Letters*, vol. 10, no. 2, pp. 378-382, Feb. 2021.
- [29] C. H. Papadimitriou and K. Steiglitz, *Combinatorial Optimization: Algorithms and Complexity*. Englewood Cliffs, NJ: Prentice-Hall Inc., 1982.
- [30] A. Ben-Tal and A. Nemirovski, *Lectures on Modern Convex Optimization: Analysis, Algorithms, and Engineering Applications*. Philadelphia, PA, USA: SIAM, 2001.
- [31] M. Grant and S. Boyd, *CVX: Matlab software for disciplined convex programming*, version 2.1, <http://cvxr.com/cvx>, March 2014.
- [32] K.C. Toh, M.J. Todd, and R.H. Tutuncu, "SDPT3 — A Matlab software package for semidefinite programming," *Optimization Methods and Software*, vol. 11, no. 1-4, pp. 545-581, 1999.
- [33] W. Hoeffding, "Probability inequalities for sums of bounded random variables," *Journal of the American Statistical Association*, vol. 58, no. 301, pp. 13-30, Mar. 1963.